SINAPSE ASM

ABSTRACT BOOK

Aberdeen, Scotland
9 June 2025

CONTENTS

KEYNOTE TALKS

IT01

The Myelin Bootstrap: New Applications of MRI

Robert Turner[1*]

1. Max-Planck Institute for Human Cognitive and Brain Sciences
   Sir Peter Mansfield Imaging Centre, University of Nottingham
   School of Psychology, Cardiff University

Abstract:

Histological studies of myelin-stained sectioned cadaver brain and in-vivo myelin-weighted magnetic resonance imaging show that the cerebral cortex is organized into cortical areas with generally well-defined boundaries, which have consistent internal patterns of myelination--their myeloarchitecture. Cortical myelinated axons can be classified into radial axons, mostly connecting excitatory pyramidal neurons to other neurons via the white matter, and tangential neurons providing intracortical connections. Recent histological studies show that many of these tangential myelinated axons arise from interneurons that stain for parvalbumin, identifying them as inhibitory neurons. Further recent discoveries have revealed that the process of myelination is largely driven in development by neural experience, such that the axonal passage of action potentials increases axonal diameter and stimulates neighbouring oligodendrocytes to perform their task of wrapping axons with myelin. This bootstrapping process, in which the traffic of action potentials facilitates increased traffic, suggests the hypothesis that the myeloarchitecture in each cortical area reveals the principal cortical microcircuits required for the function of that area, fine-tuned by experience. If this idea is correct, observation using high resolution quantitative MRI of the sequential maturation of specific brain areas throughout the lifespan, combined with unsmoothed fMRI data and dMRI tractography, can provide evidence for neuropsychological models of the stages of normal and abnormal cognitive development. Such an approach may provide objective biomarkers for the identification of different types of mental illness.

IT02

Shared Neurocognitive Patterns in Autism and Eating Disorders: Connecting the dots!

Kate Tchanturia[1*]

1. King's College London, Strand, London WC2R 2LS

Socio-emotional and cognitive difficulties are recognised as maintaining factors for eating disorders (EDs). Among EDs, anorexia nervosa (AN) is one of the most challenging to treat, with the highest mortality rate, and high risk of chronicity. Understanding underlying mechanisms and identifying treatment targets is therefore crucial. Furthermore, patients with co-occurring neurodevelopmental conditions such as autism, need adaptations to existing treatments, as these were developed for neurotypical populations.

Research on neurocognitive functioning and emotional processing has pointed to the similarities between autism and EDs. I will present findings from my lab that explores these similarities, progressing from experimental studies to ongoing neuroimiging research and future directions. The neuroimaging data from our BEACON project (Brain imaging Emotion And Cognition Of adolescents with anorexia Nervosa) may help us understand neural correlates of socio-emotional and cognitive processes in AN, with implications for treatment development and personalization.

ORAL PRESENTATIONS

OT01

In-vivo detection and treatment response assessment of rectal cancer using Field Cycling Imaging

Amnah Alamri[1,2], Nicholas Senn[1], Leslie Samuel[3], Rosalind Mitchell-Hay[4], David Lurie[1], George Ramsay[4], and Lionel Broche[1]

1. School of Medicine, Medical Sciences and Nutrition, University of Aberdeen, Aberdeen, United Kingdom.
2. Department of Radiologic Sciences, King Abdulaziz University, Jeddah, Saudi Arabia.
3. Department of Oncology, Aberdeen Royal Infirmary, Aberdeen, United Kingdom.
4. Aberdeen Royal Infirmary, Aberdeen, United Kingdom.

Relevant Keywords: rectal cancer, field-cycling imaging, chemoradiotherapy, tumour microenvironment

Abstract:

Rectal cancer is a major global health concern, and accurately assessing tumour response to neoadjuvant chemoradiotherapy (nCRT) remains a key clinical challenge (1). Fast Field-Cycling Imaging (FCI), a novel MRI-based method, offers quantitative insights into tissue microstructure by measuring the R_1 relaxation rate ($1/T_1$) across varying magnetic field strengths, without the need for contrast agents (2). In this pilot study, we investigate the potential of FCI to detect and characterise tumour response to nCRT in locally advanced rectal cancer (LARC).

Eighteen patients with LARC underwent FCI scanning before and after nCRT using a saturation recovery spin echo sequence across four evolution fields (200, 20, 2, and 0.2 mT) and five evolution times. Data sets were first denoised, followed by voxel-by-voxel fitting using custom MATLAB software to extract R_1 values. Analysis focused on comparing R_1 dispersion profiles between rectal tumours and adjacent healthy tissue, before and after treatment.

Results revealed that tumour regions consistently demonstrated higher R_1 values at lower field strengths and steeper NMRD (Nuclear Magnetic Relaxation Dispersion) slopes compared to healthy tissues (Figure 1). Post-treatment scans showed a decrease in R_1 values among responders. In contrast, minimal profile change in a non-responder highlighted the potential of R_1 slopes as sensitive indicators of treatment efficacy (Figure 2).

This is the first in vivo study applying FCI to monitor rectal cancer therapy response, demonstrating its ability to non-invasively characterise tumour microstructure and post-treatment changes. Our results showed that R_1 NMRD profiles revealed functional contrast that reflected changes related to tumour activity and potentially to extracellular matrix remodelling. Future studies incorporating multiple post-treatment imaging timepoints, could improve the ability to distinguish tumour regression from fibrotic remodelling, ultimately guiding early intervention and personalised treatment strategies.

Acknowledgement: A.A. acknowledges sponsorship from King Abdulaziz University, Jeddah, Saudi Arabia

Contact: Amnah Alamri (a.alamri.20@abdn.ac.uk).

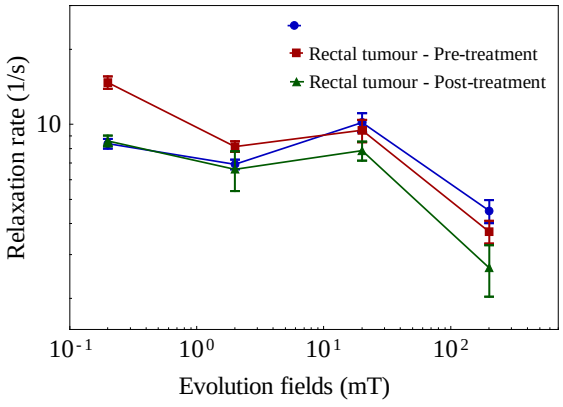

Figure 1 Average NMRD profiles of rectal tumour (pre- and post-treatment) and healthy tissue. Error bars indicate standard error of the mean (SEM).

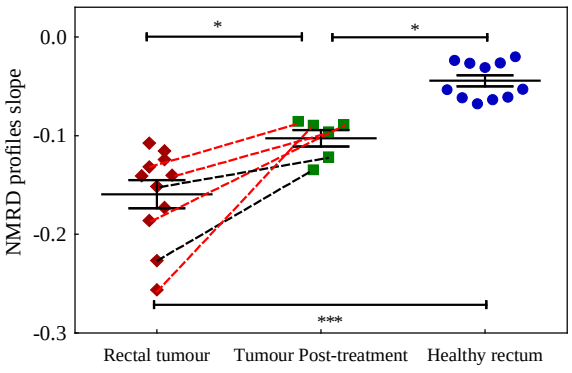

Figure 2 Comparison of NMRD slope in rectal tumour (pre/post-treatment) vs. healthy tissue. Red dashed lines: complete responders; black: partial/non-responders. *= p<0.05, ***= p<0.0005 and ns = not significant.

References:

(1) Ryan et al., Colorectal Dis., 2015;17(10):849–61. (2) Broche et al., Sci Rep., 2019;9:PMC6639535.

OT02

Effective treatment for Alzheimer's Disease proven on brain imaging

Anca-Larisa Sandu[1], Serena Lo[2,3], Nafeesa Nazlee[2], Helen Shiells[2], Bjoern Schelter[2,3], Claude Wischik[2,4], Roger T Staff[5]

1. Aberdeen Biomedical Imaging Centre, University of Aberdeen
2. TauRx Therapeutics Ltd., Aberdeen
3. Institute for Complex Systems and Mathematical Biology, University of Aberdeen
4. Institute of Medical Sciences, University of Aberdeen
5. Aberdeen Royal Infirmary NHS Grampian

Keywords: Clinical Applications, Image analysis

Abstract:

To address the health challenge of human longevity with its downsides such as Alzheimer's Disease (AD), an effective treatment for this neurodegenerative disease becomes a necessity. TauRx has focused on developing an oral treatment targeting the tau aggregation pathology of AD, hydromethylthionine (HMTM), currently submitted for regulatory approval. The goal of the current study is to determine whether HMTM has a positive effect on brain structure.
Data was obtained from 90 sites in seven countries in Europe and North America. After site qualification for quality and standardisation, structural T1-weighted images were acquired using a three-dimensional magnetization-prepared rapid gradient echo or equivalent sequences to acquire 3-DT1 images of the brain across two years. Sequence parameters were selected to match the Alzheimer's Disease Neuroimaging Initiative (ADNI) acquisition protocol.
The data analysed comprised 156 patients who had taken HMTM 16 mg/day and 41 who had taken 8 mg/day, 176 controls and 105 patients from ADNI. In the current study we used the baseline and the next time point after a year. Data were compared using the longitudinal flexible factorial design from Computational Anatomy Toolbox (CAT12). We then tested using the Statistical Parametric Mapping (SPM) interface for locations where changes (reduction in GM) in the treated groups (16 mg/day and 8 mg /day) were smaller than reductions in the control patients or ADNI patients.

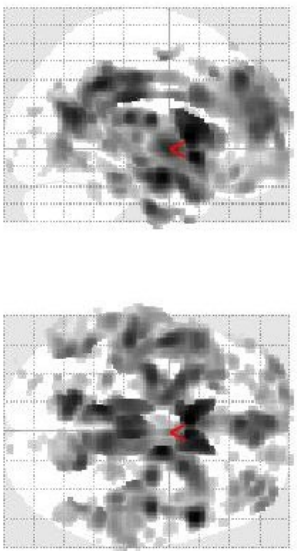

Figure A) Treatment (16mg and 8mg) minus control patients

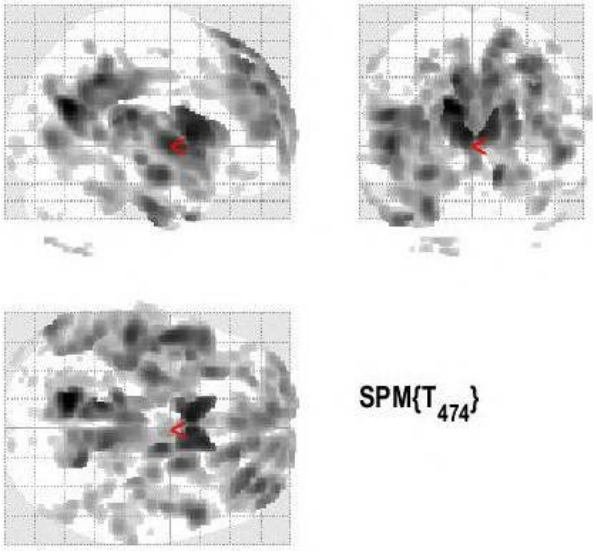

Figure B) Treatment (16mg and 8mg) minus ADNI patients

Following the standard SPM Voxel-Based Morphometry (VBM) statistical thresholding approach, a threshold of $p<0.001$ uncorrected was applied. Preliminary results suggest that subjects receiving hydromethylthionine had significantly less grey matter loss over 12 months in hippocampus and parahippocampal gyrus bilaterally, right and left temporal lobes, and parts of medial frontal lobe including anterior cingulate, regions known to be particularly affected by tau aggregation pathology. Similar results are from both comparisons when compared with trial controls or with ADNI participants.

Contact: anca.sandu-giuraniuc@abdn.ac.uk

OT03

Investigating Cardiovascular Risk as a Moderator of the Relationship between Blood Plasma Dementia Biomarkers and Cognitive Impairment – A Cross-sectional Analysis of Data from the Bio-Hermes Study

Angelina Kancheva[1*], Donald Lyall[2], Joanna Wardlaw[3], Terence Quinn[1]

1. School of Cardiovascular and Metabolic Health, University of Glasgow, UK
2. School of Health and Wellbeing, University of Glasgow, UK
3. Centre for Clinical Brain Sciences, University of Edinburgh, UK

Keywords: blood plasma biomarkers, dementia, cognitive impairment, cardiovascular risk

Abstract:

Background and Aims:

Blood plasma biomarkers have the potential to revolutionize diagnosis and prognosis of Alzheimer's disease (AD) and other dementias. As vascular risk factors contribute to cognitive impairment (CI) and dementia, we aimed to explore whether cardiovascular disease (CVD) risk moderates the relationship between blood plasma dementia biomarkers and CI.

Methods:

We included cognitively normal (CN) healthy controls and participants with mild cognitive impairment or probable AD (CI group) from the Bio-Hermes study. Clinical presentation of CN or CI was determined based on clinical screening procedures. CVD risk was calculated using the Atherosclerotic CVD (ASCVD) risk score calculator. We conducted a series of logistic regression analyses to evaluate the association of each of several AD biomarkers (plasma amyloid beta (Aβ) 42/Aβ40, phosphorylated tau (p-tau)181, p-tau217, apolipoprotein E gene ε4 allele (Apoε4) status) and CVD risk, with CI. We then tested moderation by CVD risk in each model.

Results:

We included 745 participants (301 CN, 444 CI; mean age 72.3 years; 56.8% female). In each model, blood plasma biomarkers and CVD risk were significantly associated with CI. Strongest association was for p-tau217 (OR=2.33 [95%CI:1.89-2.9]). CVD risk did not significantly moderate the relationship between blood plasma biomarkers and CI.

Conclusions:

In our study, blood plasma dementia biomarkers and CVD risk significantly associated with CI, but CVD risk did not significantly moderate the relationship between plasma biomarkers and CI. Plasma biomarkers and CVD risk might confer independent risk of CI. Given the multiple risk factors for dementia and large implications for social and healthcare systems globally, CVD risk assessment should complement other dementia biomarker assessments.

Acknowledgements:
Data for this study were provided by the study sponsor Global Alzheimer Platform Foundation (GAP), and accessed as part of the Scottish Data Challenge using an Alzheimer's Disease Data Initiative (ADDI) workspace.

Contact: 2832547K@student.gla.ac.uk

OT04

A large brain imaging dataset for dementia research: a Scottish Medical Imaging (SMI) cohort

Michael Camilleri[1,2,3], Dorian Gouzou[2], Salim Al-Wasity[4], Bea Alex[3], Alex Doney[4], **Maria Valdés Hernández[2,5]**, Susan Krueger[4], Douglas Steele[4], Emanuele Trucco[1], Sotos Tsaftaris[6], Joanna Wardlaw[2,5], William Whiteley[2,7]

1. School of Science and Engineering, University of Dundee, UK
2. Centre for Clinical Brain Sciences, University of Edinburgh, UK
3. School of Informatics, University of Edinburgh, UK
4. School of Medicine, University of Dundee, UK
5. UK Dementia Research Institute, University of Edinburgh, UK
6. School of Engineering, University of Edinburgh, UK
7. Health Data Research UK

Keywords: image analysis, natural language processing, Scottish National Safe Heaven, dementia research, brain MRI

Abstract:

Introduction:

Large, representative brain imaging datasets with very long-term follow up are needed to advance dementia prediction. We propose a method using data collected during routine clinical care, linked to electronic health records (EHR) to address this need.

Methods:

We identified brain CT and MRI from SMI dataset and linked the (pseudo-anonymised) subjects to their EHR in NHS Scotland. Machine-learning of meta-data and voxels, coupled with natural language processing of the text-reports, identified imaging sequence, body part, and major abnormalities. EHR were used to identify dementia subtypes and other diseases with ICD10 and drug code lists from general and mental health hospital admission, and death and prescription records. All analysis was performed in the secure Scottish National Safe Haven (NSH).

Results:

Between 2008−2018, 830,884 people (449,447, 54% female) had ≥ 1 brain MRI [294,422, 34%] or CT [669,539, 81%]. The mean age [and follow-up] from first scan (in years) was 62 [7.3] for CT and 53 [6.9] for MRI. During follow-up, any dementia was recorded for 16,819 (6%) people with an MRI scan, and 119,423 (18%) with CT. People with dementia had at least one record of unspecified dementia [58%], Alzheimer's disease, [53%] vascular dementia [37%] or rarer causes [4%]. Following quality-assessment checks (reports of tumour/haemorrhagic stroke, unclear diagnosis, <40 at scan, limited follow-up), we identified 10,709 dementia patients with an MRI and 57,242 equivalent CT subjects: these were sex and age (at scan) matched to the same numbers of healthy controls.

Conclusions:

We curated a proof-of-concept brain imaging dataset for neurodegenerative diseases research and practice. Provision of such data should be a priority for secure data environments across the UK, to support development of Artificial Intelligence (AI) techniques for disease prediction and modelling.

Acknowledgements:
This work is supported by NEURii, a collaborative partnership involving the University of Edinburgh, Gates Ventures, Eisai, LifeArc and Health Data Research UK (HDR UK). We acknowledge the eDRIS team (Public Health Scotland) for their support in obtaining approvals, the provisioning and linking of data and facilitating access to the NSH.

Contact: M.Valdes-Hernan@ed.ac.uk

OT05

Stroke Diagnosis from Field-Cycling Imaging using Machine Learning

Adamu Ali-Gombe[1], Nicholas Senn[1], Lionel M. Broche[1], Vasiliki Mallikourti[1], P. James Ross[1], Mary Joan Macleod[1 *], Gordon Waiter[1]

1. Aberdeen Biomedical Imaging Centre, The Institute of Medical Sciences, School of Medicine, Medical Sciences and Nutrition, University of Aberdeen, UK

Keywords: Field-Cycling Imaging (FCI), Vision Transformer (ViT), Image Analysis, Stroke, Area Under Curve (AUC)

Abstract:

Background:

Recent advances in Field-Cycling Imaging (FCI) have demonstrated its potential in stroke diagnosis using quantitative measures such as R_1 dispersion. This first proof-of-concept study aimed to determine if a machine learning model can detect the presence of stroke in FCI images and whether the model can distinguish between hemorrhagic and ischemic stroke in patients.

Methods:

The dataset consisted of thirteen stroke patients (5 hemorrhagic, 8 ischemic) and seventeen volunteers without a stroke present, all scanned using FCI at 0.2, 2.0, and 20 mT at five evolution times (5ms to 550ms), resulting in fifteen images per individual. Participants were scanned shortly after their stroke and approximately thirty days after the initial scan. The data was split into training and test sets based on the initial and follow-up scans. The first experiment was conducted on all 15 images. The second and third experiments were run on two image sets grouped by evolution times - shorter and longer evolution times (Figure 1). A pre-trained Vision Transformer was used to extract learnable class features, and an SVM was then trained on those features. Performance was evaluated using accuracy and AUC.

Results:

When differentiating between stroke and non-stroke participants, the best performance was achieved when the model was trained on longer evolution time images, reaching 85% accuracy and an AUC of 0.94 (Figure 2a). When the model was trained to classify ischemic and hemorrhagic strokes, an accuracy of 84% and an AUC of 0.91 was obtained (Figure 2b).

Conclusion:

This initial study showed that learned class features from FCI images possess discriminative properties that differentiate a stroke from a non-stroke patient within the limited data. Additionally, these features can be utilised to differentiate between ischemic and hemorrhagic strokes. Future work will focus on multi-task models for detecting various brain-related frailties in FCI images.

Acknowledgements:

This work is supported by the Chief Scientist's Office (Grant number TCS/19/44, TCS/24/05).

Contact: adamu.ali-gombe@abdn.ac.uk

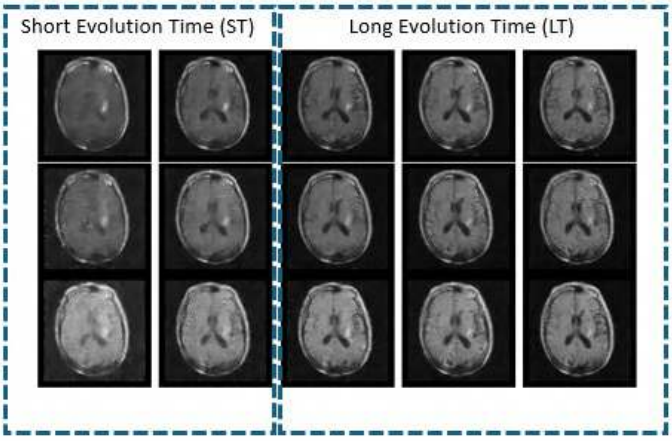

Figure 1: Images from a single scan across all field strengths are presented, grouped by evolution times. On the left is the first group of images with shorter evolution times(ST), and on the right is the second group of images with longer evolution times (LT).

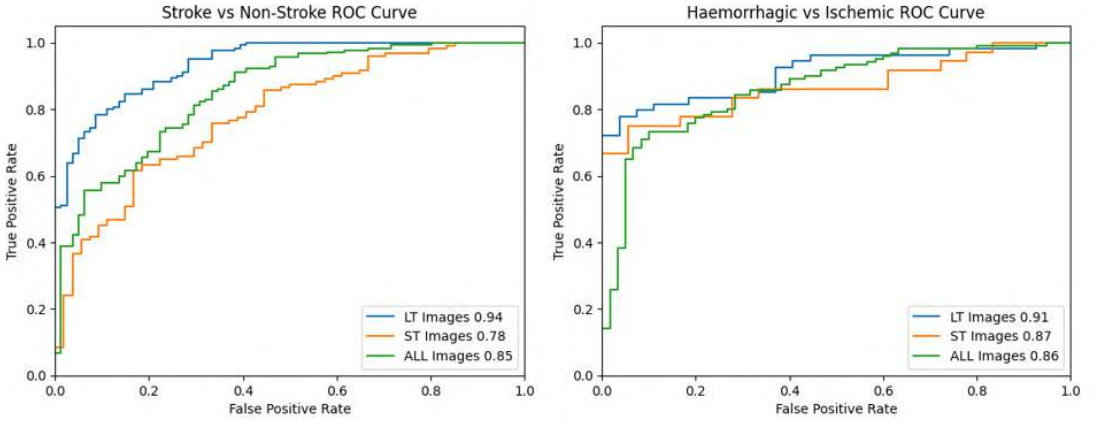

(a) (b)

Figure 2: a. ROC curve for stroke versus non-stroke participants, b. ROC curve for haemorrhagic versus ischemic. LT refers to longer evolution time images, ST denotes shorter evolution time images, and ALL represents all images from the slices.

OT06

The use of statistical shape modelling to identify a morphological marker of hippocampal atrophy from a single MRI scan

McNeil C.J[1], Sandu A[1], A Murray[1], Waiter G[1]

1. Aberdeen Biomedical Imaging Centre, Institute of Medical Sciences, School of Medicine, Medical Sciences and Nutrition, University of Aberdeen, UK

Keywords: MRI, shape analysis, cohort, hippocampus

Abstract:

Hippocampal volume is influenced by both intracranial volume (ICV), and by atrophy with age or due to neurodegenerative disease. ICV is influenced by sex, genetics and the environment with brain/ICV ratio maximal by 25y. Brain atrophy within a constant ICV begins during mid-life and continues until death. Identifying people whose hippocampi have undergone accelerated atrophy would aid the diagnosis of neuropathologies including Alzheimer's disease.

We examined how the morphology of the hippocampi vary with age and ICV. Volume differences related to age are predominantly caused by atrophy, intra-individual change, whereas differences with ICV are related to inter-individual variation in head size. We hypothesised that some atrophy related morphological differences are distinct from those related to ICV.

831 members of the STRADL cohort (26-82y, $\bar{X}$ = 60y) underwent MRI, and hippocampi segmented using the Freesurfer software. These were analysed with the ShapeWorks Studio software using particle-based modelling to quantify morphology (1). We used principle component analysis to reduce the geometric data to shape representations suitable for traditional statistical analysis. The morphology, size and relative position of the hippocampi of each participant can be described using these principle components which can be conceptualized as shape characteristics (SCs). The effect of age and ICV on fifty SCs were analysed by regression, and p-values were corrected using the False Discovery Rate method.

Fifty SCs captured 99.6% of the total shape variation of the sample. Age and ICV were jointly associated with 3 SCs. ICV was uniquely associated with 8 SCs. Age was uniquely associated with one SC ($p=1.3 \times 10^{-12}$) and correlated with age ($R^2=0.07$). When visualising this SC, it showed a thinning, without shortening, of both hippocampi as age increased.
We have identified an age-related morphological change of the hippocampi that is a strong candidate marker of hippocampal atrophy.

Figure 1. Montage of SC12 morphological difference. -3 SD to +3 SD. Positively correlated with age.

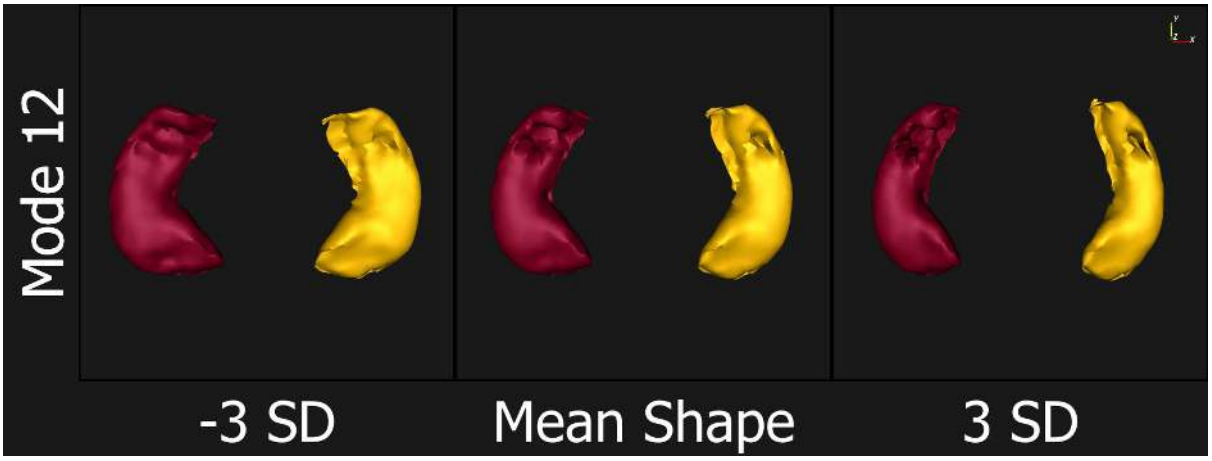

Reference

(1) Joshua Cates, Shireen Elhabian, Ross Whitaker. "Shapeworks: particle-based shape correspondence and visualization software." Statistical Shape and Deformation Analysis. Academic Press, 2017. 257-298.

Contact: c.mcneil@abdn.ac.uk

OT07

Modified CBAM: Sub-Block Pooling for Improved Channel and Spatial Attention

Hamza Hussaini[1*], Shahana Bamo[1], Eyad Elyan[1], Carlos Moreno-Garcia[1]

1. Robert Gordon University, Garthdee Road, Aberdeen, AB10 7QB, Aberdeen, United Kingdom.

Keywords: Modified Convolutional Block Attention Module (MCBAM), Convolutional Block Attention Module (CBAM), Convolutional Neural Network (CNN), Attention Mechanisms, Medical Imaging, Global Pooling, Sub-block Pooling, Channel Attention, Spatial Attention, Leukemia, Blood Cells, Chest X-Ray.

Abstract:

The Convolutional Block Attention Module (CBAM) has emerged as a widely adopted attention mechanism, as it seamlessly integrates into the Convolutional Neural Network (CNN) architecture with minimal computational overhead. However, its reliance on global average and maximum pooling in the channel and spatial attention modules leads to significant information loss, particularly in scenarios demanding fine-grained feature analysis, such as medical imaging. This work proposes the Modified CBAM (MCBAM) to address this critical limitation. This novel framework eliminates the dependence on global pooling by introducing a sub-block pooling strategy that captures nuanced feature relationships, preserving critical spatial and channel-wise information. MCBAM iteratively computes attention maps along channel and spatial dimensions, adaptively refining features for superior representational power. Comprehensive evaluations on diverse datasets, including medical imaging datasets such as C-NMC (acute lymphoblastic leukemia), PCB (peripheral blood cells), and COVID-19 (Chest X-ray), as well as the non-medical KMNIST for validation, demonstrate the efficacy of MCBAM in different scenarios. Additionally, we evaluate MCBAM against similar alternatives, such as the Bottleneck Attention Module (BAM), Normalisation-Based Attention Module (NAM), and Triplet Attention Module (TAM), demonstrating that MCBAM consistently outperforms these advanced attention mechanisms across all datasets and metrics. Furthermore, results reveal that MCBAM surpasses the standard CBAM and establishes itself as a robust and effective enhancement for attention mechanisms, with notable improvements in medical imaging tasks, offering critical advantages in complex scenarios.

Contact: h.hussaini@rgu.ac.uk

OT08

A Systematic Review of Cerebrovascular Reactivity Delay Assessment in Gas-Challenge Blood-Oxygen-Level-Dependent Magnetic Resonance Imaging

Keelin N. Ridge[1,2*], Joanna M. Wardlaw[1,2], Michael J. Thrippleton[1,2], Michael S. Stringer[1,2]

1. Centre for Clinical Brain Sciences, University of Edinburgh, United Kingdom
2. UK Dementia Research Institute at the University of Edinburgh, United Kingdom

Keywords: MRI**,** systematic review, image analysis, methods development, neuroimaging

Abstract:

Background:

Cerebrovascular reactivity (CVR), the ability of cerebral blood vessels to respond to vasoactive stimuli, is an important marker of vascular health. CVR can be measured via blood-oxygen-level-dependent (BOLD) MRI during gas administration. While CVR magnitude is well-established, CVR delay and similar temporal characteristics remain under-researched. A lack of standardised methodologies and definitions for CVR delay limits its potential as an indicator of neurovascular integrity. We conducted a systematic review to identify studies assessing temporal CVR features, summarising key findings and highlighting gaps in the existing literature.

Methods:

We systematically searched EMBASE, MEDLINE, Web of Science, and Institute of Electrical and Electronics Engineers Xplore for human CVR studies (January 1990-2024) using gas-challenge BOLD-MRI that explicitly accounted for temporal features of the BOLD response. One author performed title/abstract and full-text screening, with eligibility queries resolved by discussion. We extracted data encompassing demographics, MRI parameters, paradigm features, delay computation methods, reported delay values, and findings.

Results:

We identified 172 relevant studies (4171 participants: 2736 patients, 1435 healthy individuals). Only 35 studies (20%) reported numerical delay values. Cross-correlation was the most popular delay computation technique, followed by iterative delay-to-plateau determination, linear regression, and haemodynamic response function fitting (Figure 1). Studies researching the validity of delay-type measures were limited. Among 126 pathology-focused studies, longer delays were observed in patients versus controls in steno-occlusive disease, sickle cell disease, and Alzheimer's disease (Table 1). Findings varied in other pathologies, potentially due to differing experimental/processing protocols and within-disease variability.

Discussion/Conclusion:

This systematic review highlights the lack of standardised methods for assessing CVR delay using gas-challenge BOLD-MRI, despite numerous studies linking delay to disease severity across various pathologies. Inconsistent reporting, heterogeneous delay computation techniques, and limited understanding of delay validity emphasise the need for further research and consensus to help establish CVR delay as a robust vascular biomarker.

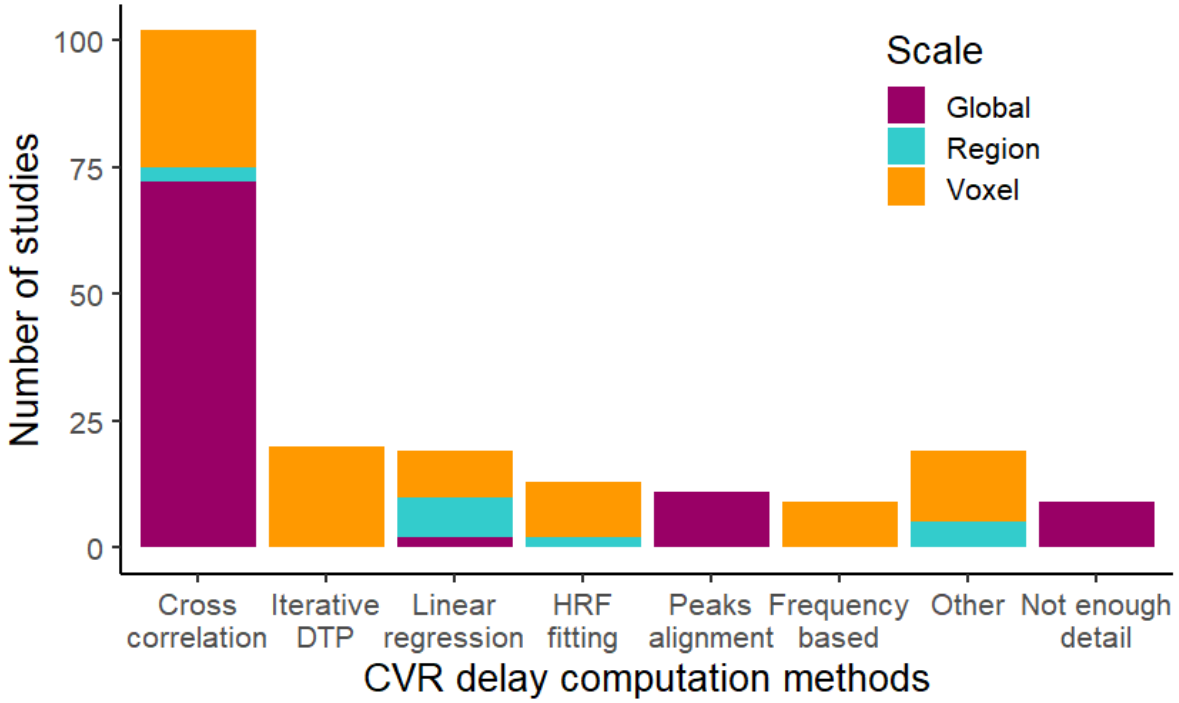

Figure 1. Distribution of delay methodologies and computational scales across 172 studies. 'Other' encompasses deconvolution, carpet-plot analysis, non-linear model fitting, and including temporal derivatives in linear modelling.
DTP = delay-to-plateau, HRF = haemodynamic response function.

		CVR delay: patients relative to healthy controls		
		Shorter	**No difference**	**Longer**
CVR magnitude: patients relative to healthy controls	**Higher**	Concussion = 2 studies		Traumatic brain injury = 1 study
	No difference		Mild cognitive impairment = 1 study	Mild cognitive impairment = 1 study Alzheimer's disease = 2 studies
	Lower	Small vessel disease = 1 study	Steno-occlusive disease = 1 study Normal ageing = 1 study CADASIL = 1 study	Normal ageing = 2 studies Parkinson's disease = 1 study Sickle cell disease = 2 studies Steno-occlusive disease = 3 studies Small vessel disease = 1 study

Table 1. Differences in CVR delay between patients and controls across 18 studies comparing measurements in healthy and patient groups.

CADASIL = Cerebral autosomal dominant arteriopathy with subcortical infarcts and leukoencephalopathy.

Acknowledgements:
This work is supported by the Precision Medicine DTP grant (MR/N013166/1) and the Row Fogo Centre (Row Fogo 6).

Contact: Keelin.Ridge@ed.ac.uk

OT09

Fast Field-Cycling as a Tool for Investigating Fibrin Clot Microstructure

Madeleine Rhodes[1*], NJ Mutch[1], and Lionel M. Broche[1]

1. Institute of Medical Science, School of Medicine, Medical Sciences and Nutrition, Aberdeen, AB252ZD, United Kingdom

Keywords: Relaxometry, microstructure, mathematical modelling, fibrin clot

Abstract:

Fast field-cycling NMR relaxometry (FFC-NMR) uses varying low magnetic field strengths (250 mT to 2 μT) to measure the T1 of materials, including biological systems (Figure 1). These measurements provide nuclear magnetic resonance dispersion (NMRD) profiles that reflect molecular dynamics of water occurring on different timescales (ms to μs). However, the meaning of these measurements is unclear in biological systems.

We explored the use of fibrin gels to determine biologically relevant properties of NMRD profiles for fibrous structures. In fibrin clots, water molecules exhibit many dynamics, including adsorption and desorption and reorientation mediated by translational displacements (RMTD). RMTD depends on the water diffusion constant and fractal dimension and provides a model of T1 relaxation with the resonance frequency.

To determine if RMTD was dominant in the NMRD profiles of fibrin clots, we compared the fractal dimension obtained using the RMTD expression with the one obtained from confocal microscopy images. Fibrin clots were generated with various concentrations of thrombin (0.01–1 U/mL) and fibrinogen (1–3 mg/mL) and their NMRD profiles measured between 25 and 40°C across 15 different magnetic fields. The RMTD was used to extract the fractal dimension and compared with values obtained from confocal microscopy (Figure 2).

Fractal dimensions derived from RMTD expression (1.70 ± 0.1) closely aligned with microscopy results (1.68 ± 0.09) for the section of NMRD profiles between 10 mT and 100 μT ($p > 0.05$), for all fibrin and thrombin concentrations and for all temperatures.

The microstructure of fibrin clots can therefore be characterised from the NMRD profiles using RMTD, and the relaxation range between 10 mT and 100 μT reflects rapid water adsorption and desorption on the surface of fibrin fibres. This insight highlights potential use of low-field imaging of blood clots and shows that more information may be available at other frequency regimes.

References:

1. R. Kimmich and E. Anoardo. Field-cycling NMR relaxometry. Progress in Nuclear Magnetic Resonance Spectroscopy. 2004;4(3-4):257-300.

2. T. Zavada and R. Kimmich. Surface fractals probed by adsorbate spin-lattice relaxation dispersion. Physical Review. E, Statistical Physics, Plasmas, Fluids, and Related Interdisciplinary Topics. 1999;59(5):5848-5854.

Figures:

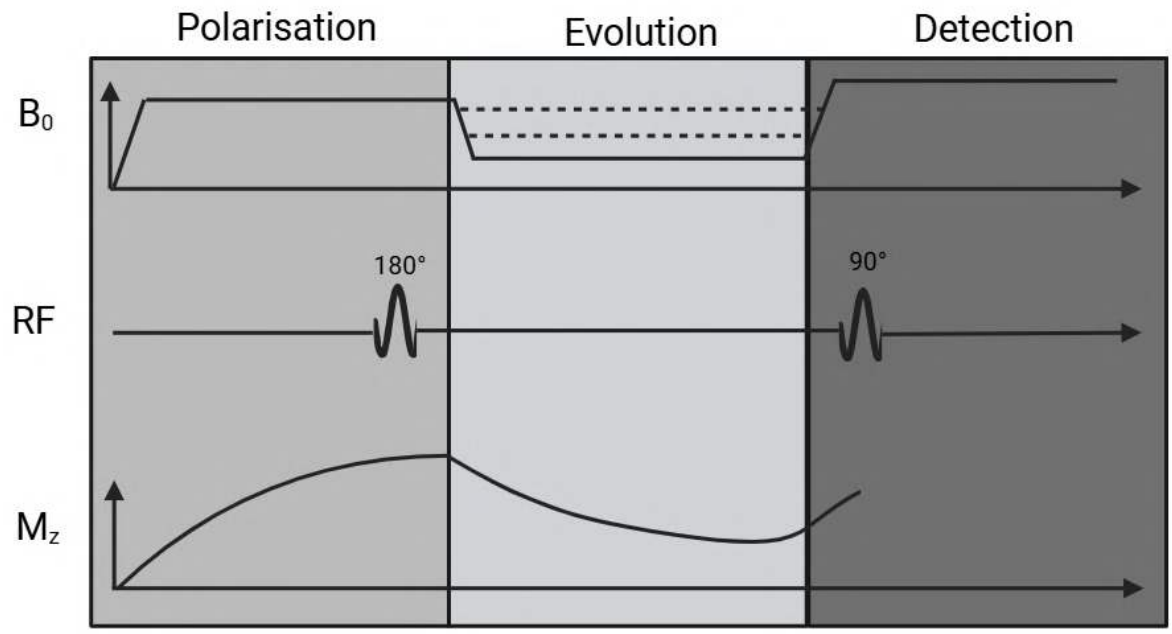

Figure 1. Fast field-cycling NMR relaxometry pulse sequence diagram. The polarisation period is used to build up magnetisation, then a 180-degree pulse inverts the spin system, which is exposed to an evolution field. Before they relax to equilibrium, a 90-degree pulse is used to detect the NMR signal and evaluate the magnetisation decay. The procedure is repeated using various evolution times and field strengths between 250 mT to 2 µT.

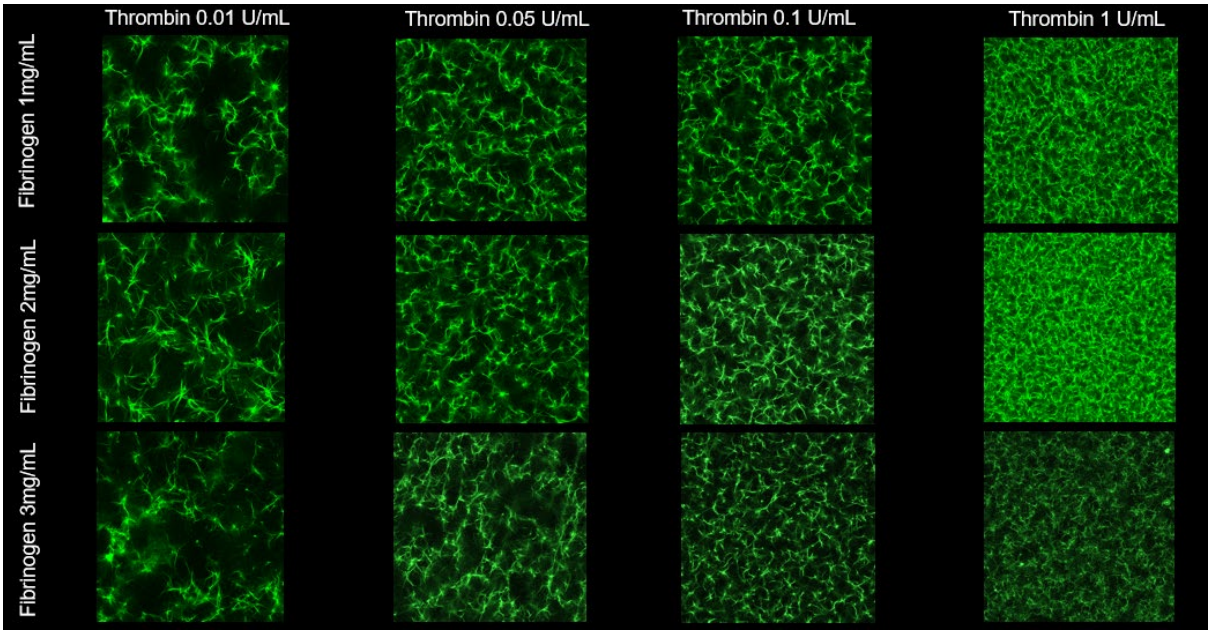

Figure 2. Confocal microscopy images of all fibrin clots. Green fluorescence represents fibrin fibres as fibrinogen was labelled with Alexa 488. Clots were imaged using x63 oil immersion objective and Ziess Airyscan 880 confocal microscope. Fibrin clots formed under high concentrations of thrombin and fibrinogen are denser and contain more fibres. These denser, more geometrically complex clots exhibit higher fractal dimensions.

Acknowledgements:

This research was funded by European Union HORIZON-MSCA-DN-2021 project FC-RELAX no. 101072758. The authors declare no competing financial interest.

Contact: Madeleine Rhodes - madeleine.rhodes@abdn.ac.uk

OT10

Evaluating the potential of *cis*- and *trans*-4-[^{18}F]fluoro-L-proline positron emission tomography as biomarkers of active collagen biosynthesis in cardiometabolic diseases

Angus K. Jacobs[1], Victoria J. M. Reid[1,2], Islay Cranston[1,2], Carlos J. Alcaide-Corral[1,2], Callum Sutherland[1], Heeyoun Hur[1], Adrian Thomson[1], Timothy J. Kendall[3], Timaeus E. F. Morgan[1,2], Kerry M. O'Rourke[1,2], Leanne M. Riley[4], Andrew Sutherland[4], Mark G. Macaskill[1,2], David E. Newby[1,2], Laura Denby[1], Jonathan A. Fallowfield[3], Adriana A. S. Tavares[1,2]

1. Centre for Cardiovascular Science, The University of Edinburgh, UK
2. Edinburgh Imaging, The University of Edinburgh, UK
3. Institute for Regeneration and Repair, The University of Edinburgh, UK
4. School of Chemistry, University of Glasgow, UK

Keywords: Preclinical PET, Systems-based imaging, Cardiometabolic disease, Collagen metabolism, Fibrosis

Abstract:

The increased prevalence of obesity and its associated comorbidities has coincided with an upsurge in cardiometabolic diseases, such as heart failure with preserved ejection fraction, metabolic dysfunction-associated steatotic liver disease, and chronic kidney disease. Active tissue remodelling and fibrosis following cellular damage and inflammation, characterised by aberrant collagen deposition, is a common feature of cardiometabolic disease. Currently, there are no established probes for non-invasive whole-body imaging of active collagen biosynthesis to study the multisystem consequences of cardiometabolic diseases. We aimed to evaluate the potential of *cis*- and *trans*-4-[^{18}F]fluoro-L-proline positron emission tomography (PET) as biomarkers of active misfolded and stable triple helical collagen biosynthesis, respectively, using a preclinical Western-style diet (WD)-induced rat model of cardiometabolic diseases. Animals fed a WD had significantly greater uptake of both *cis*- and *trans*-4-[^{18}F]fluoro-L-proline in the heart compared to age-matched controls across the time course, reflecting the increased histological accumulation of collagen, a profibrotic gene expression profile, and cardiac dysfunction on echocardiography. Although histological and transcriptional alterations were also noted in the liver, there were no detectable differences in hepatic *cis*- and *trans*-4-[^{18}F]fluoro-L-proline PET signal. We hypothesise that the organ-specific differences in relative [^{18}F]fluoro-L-proline PET uptake reflect disease-associated perturbations to the free-proline pool. Previous reports showed that WD feeding markedly increased the proline content of plasma and liver tissue[1] which could in turn alter tracer kinetics. Currently, we are developing and validating new quantification strategies for [^{18}F]fluoro-L-proline PET studies based on amino acid blood concentrations, similar to established plasma glucose corrections in [^{18}F]fluorodeoxyglucose PET studies[2], in order to improve [^{18}F]fluoro-L-proline PET outcome reporting. Overall, our data suggests that the rates of active collagen biosynthesis in cardiometabolic diseases are organ-specific, likely indicating differences in susceptibility to injury and fibrosis.

1. Tu, Honghu et al. "Glutaminase 1 Blockade Alleviates Nonalcoholic Steatohepatitis via Promoting Proline Metabolism." Biochemical and biophysical research communications. 634 (2022): 1–9. Web.
2. Boellaard, Ronald et al. "FDG PET/CT: EANM Procedure Guidelines for Tumour Imaging: Version 2.0." European journal of nuclear medicine and molecular imaging 42.2 (2015): 328–354. Web.

Acknowledgements
This work is supported by the British Heart Foundation.

Contact: angus.jacobs@ed.ac.uk

OT11

Investigating the feasibility of centre-out 3D radial MRI at low-field (0.1T) for self-navigated reconstruction of spontaneous breathing lung

Nicholas Senn[1*], Gabriel Zihlmann[1], Mathieu Sarracanie[1], and Najat Salameh[1]

1. Center for Adaptable MRI Technology (AMT Center), Institute of Medical Sciences, School of Medicine, Medical Sciences & Nutrition, University of Aberdeen, UK

Keywords: MRI, Low-field MRI, Radial Lung, Image reconstruction

Abstract:

Beyond standard methods for measuring global respiratory function of the lung, new developments in 3D MRI spirometry make it possible to measure variations in structure and function across the lung[1,2]. This involves acquiring imaging data during spontaneous free breathing using 3D centre-out radial-based approaches (Kooshball MRI), and analysis of the images reconstructed to cover the breathing cycle through self-navigation [3]. Because accessibility to high-field MRI systems can be a true challenge, we investigate the feasibility of Kooshball MRI at very-low field (0.1T) for self-navigated reconstruction as a first step towards more accessible 3D lung spirometry [4].

Imaging experiments were performed using a non-commercial, 0.1 T resistive whole-body scanner. A 3D unbalanced gradient echo sequence was used to acquire 60,000 centre-out radial trajectories, with TE/TR of 0.67/14 ms, voxel size 3.1x3.1x3.1 mm^3, AZTEK trajectory pattern of 1-twist, 1-shuffle, 4-speed, and scan time of 14 minutes. Data was collected from a test phantom object (Fig. 1B) with the scanner bed manually displaced with an amplitude of 30 mm and approximate period of 5 seconds [3]. Two additional datasets were collected consecutively (120,000 spokes) from a single healthy volunteer who was instructed to follow a consistent, slow breathing pattern. A simple gridding-based reconstruction scheme was deployed using MATLAB.

The periodic movement of the phantom and lung was observable (Fig. 1C) as a periodic variation of the DC magnitude signal (i.e., the centre of *k*-space). A total displacement of 59 ± 6 mm and 28 ± 6 mm was measured between the first and final images of moving phantom and diaphragm (Fig. 2).

The feasibility of Kooshball MRI at very-low field for self-navigated reconstruction of spontaneous breathing lung was demonstrated at 0.1 T. Future work will look to further tailor the radial trajectory pattern, shorten acquisition time, and utilise more advanced image reconstruction approaches.

References:

1. Boucneau T, et al. 3D magnetic resonance spirometry. Sci Rep. 2020;10(1):9649.
2. Mendes Pereira L, et al. UTE-SENCEFUL: First results for 3D high-resolution lung ventilation imaging. Magnetic resonance in medicine. 2019;81(4):2464–2473
3. Boucneau T, et al. AZTEK: Adaptive zero TE k-space trajectories. Magnetic resonance in medicine. 2021;85(2):926–935.2.
4. V|LF Sprio3D Project Website: v-lf-spiro3d.eu

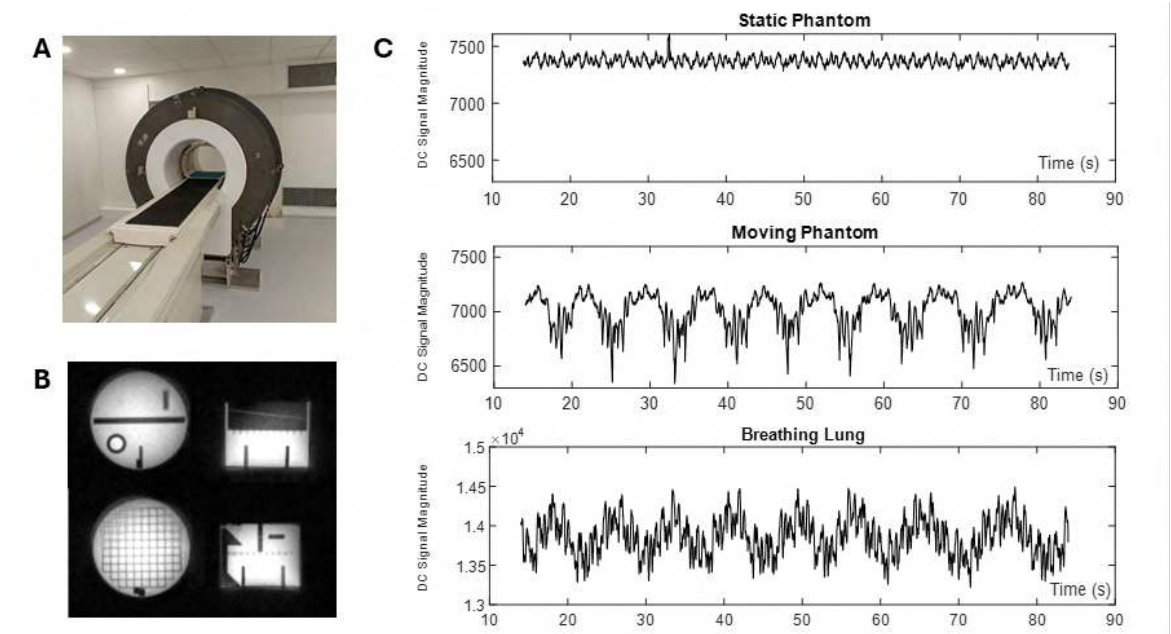

Figure 1. A: The whole-body resistive scanner that can be ramped to fields strengths ≤ 0.1 T. B: Reconstructed image of non-moving American College of Radiology (ACR) phantom using all 60,000 radial spokes. C: DC magnitude signal used for self-navigated reconstruction of the separate motion state images. 5,000 spokes acquired from non-moving phantom, moving phantom, and health volunteer free breathing lung are shown.

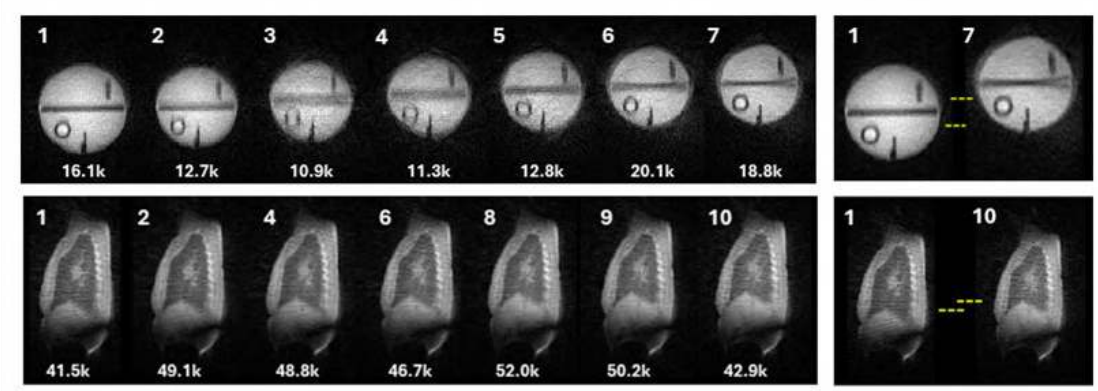

Figure 2. A total of 7 and 10 motion states were reconstructed from the phantom and lung images respectively. The number of radial spokes used for each self-navigated motion state reconstruction are shown.

Acknowledgements:

Part of the V|LF-Spiro3D project. This project has received funding from the European Union's Horizon Europe research and innovation programme under grant agreement No 101099934, and from Innovate UK grant number 10063498.

Contact: nicholas.senn2@abdn.ac.uk

OT12

Leveraging Open-Source M/EEGs to Identify Oscillatory Changes in Parkinson's Disease

Hamzeh Norouzi [1], Magdalena Ietswaart[1], Jason Adair[2] & Gemma Learmonth[1]

1. Division of Psychology, University of Stirling
2. Computing Science and Mathematics, University of Stirling

Keywords: Open Science, M/EEG, Parkinson's disease, Meta-analysis

Abstract:

Parkinson's disease is characterised by a range of motor and non-motor changes that can negatively impact quality of life. Many studies have identified potential clinical electrophysiological biomarkers of Parkinson's disease with an aim of developing new methods of identifying at-risk patients, and to form the basis of therapeutic interventions. However, there are logistical challenges in recruiting large clinical groups for cognitive neuroimaging research studies. Such limitations reduce statistical power, increase the risk of misinterpretation, and may fail to account for the substantial heterogeneity in symptom presentation and disease progression that is characteristic of Parkinson's disease. Publicly available datasets offer a powerful solution to these challenges and enable data aggregation and meta-analysis. In our recent study, we conducted a re-analysis and meta-analysis of open-source M/EEG datasets and aimed to identify consistent electrophysiological markers of Parkinson's disease. We compared periodic and aperiodic characteristics of 6 resting-state M/EEG datasets (4 EEG and 2 MEG) in 390 patients with Parkinson's disease and 607 age-matched healthy controls. Compared with controls, Parkinson's patients showed consistently higher peak alpha power and slower peak alpha frequency, along with heightened aperiodic offset and exponents, but no difference in peak beta power or frequency. This large cohort meta-analysis points to a relatively consistent pattern of both periodic and periodic changes in M/EEG signal that may be used to develop diagnostics and interventions in the future.

Acknowledgements
This work is supported by a University of Stirling Institute for Advanced Studies (IAS) PhD studentship.

Contact: Hamzeh.Norouzi@stir.ac.uk

OT13

Ethical Complexities and Concerns Surrounding Magnetic Resonance Imaging and the Open-Access Scientific Framework in Autism Research

Michelle Sader[1,2#], Ellen Maloney[2,3#], Gordon Waiter[1,2], Jess Kerr-Gaffney[2,4], Kate Tchanturia[2,4], Karri Gillespie-Smith[2,3], Fiona Duffy[2,3,5]

1. School of Medicine, Medical Sciences and Nutrition, University of Aberdeen, UK
2. Eating Disorders and Autism Collaborative (EDAC), University of Edinburgh, UK
3. School of Health & Social Sciences, University of Edinburgh, UK
4. Department of Psychological Medicine, King's College London, UK
5. NHS Lothian Child and Adolescent Mental Health Services, Royal Edinburgh Hospital, UK

[#]Authors contributed equally to this work

Keywords: Autism, MRI, Ethics, Concerns, Open-Science

Abstract:

Background:

There is increasing demand for publicly funded research datasets to be made available for the research community. However, there are multiple issues associated with the use of accessible data, particularly in the Autistic community, where individuals have understandable reservations as to who is accessing this data, what the associated objectives are regarding use of data, and why there is insufficient follow-up to individuals who have offered their time to provide their data. These issues particularly extend towards brain imaging research, in which Autistic individuals have expressed longstanding ethical concerns as to how and why this research is performed.

Methods:

This study uses discussions from a series of Autistic lived-experience panel workshops to outline concerns from the Autistic community in relation to both magnetic resonance imaging (MRI) and the functionality of the open-access scientific framework, utilising these approaches as examples to outline discipline-wide concerns and barriers to ethical research.

Results:

This work addresses a bias in research regarding who can reasonably tolerate an MRI scan as an Autistic person, and debates whether certain Autistic characteristics are being disproportionally highlighted and/or suppressed through these research practices. Lastly, this work focuses on methods with which MRI, open-science philosophy and general research disciplines can improve practice to conduct ethical autism research.

Conclusion:

As the utility of research datasets/repositories rises, researchers become increasingly responsible for managing this data and framing their research. By adopting practices recommended by individuals with lived experience, researchers can better respect the autonomy and preferences of Autistic individuals, leading to more inclusive and ethical research outcomes.

Images/Figures:

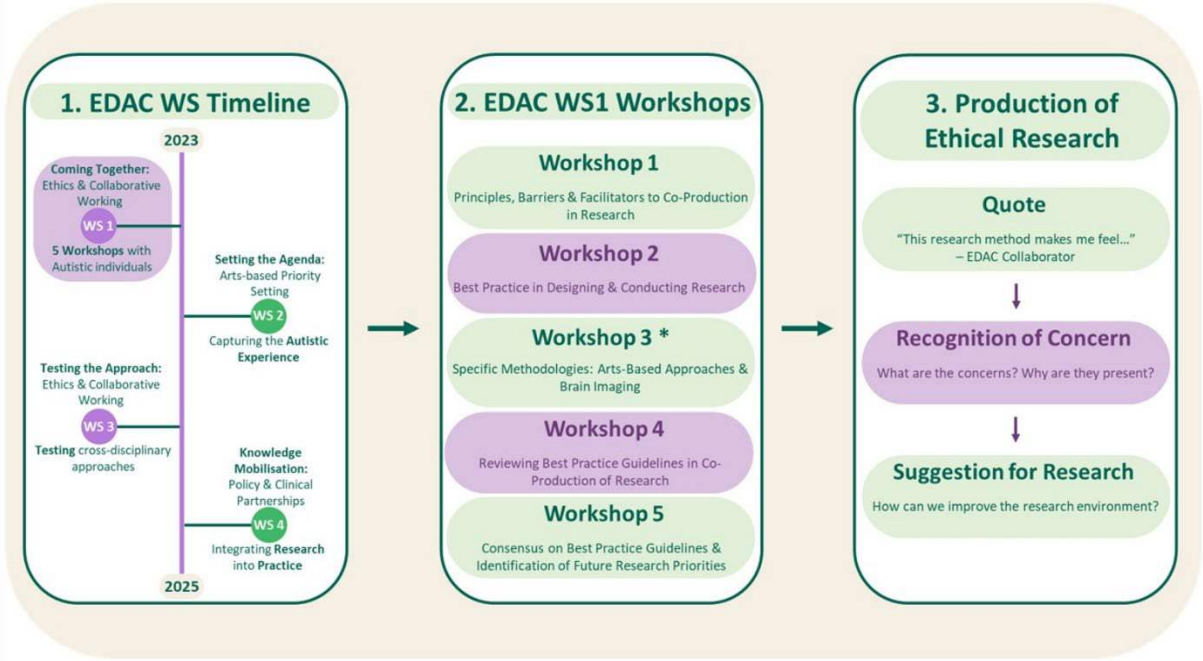

Figure 1. Visual detailing 1. the EDAC research network's WS timeline; 2. the five EDAC WS1 workshops; 3. the use of transcript material from the workshops, which led to quotes discussing how to ethically co-produce and guide priorities for autism research. The material used for this perspective piece has been derived from "WS1 – Coming Together". This image has been adapted from Duffy & Gillespie-Smith et al. (2024).21

* – Transcripts from workshop 3 were predominantly used for this piece, but transcripts from all five workshops were also incorporated into the current perspective piece.

[Abbreviations: EDAC – Eating Disorders and Autism Collaborative; WS – Work Stream]

Acknowledgements:

M.S., E.M., G.W., K.G.S and F.D are supported by UK Research and Innovation (MRC, ESRC, AHRC), the National Institute for Health and Care Research and the Medical Research Foundation as part of the EDAC network (grant number: MR/X03058X/1). KT and JKG are supported by the National Institute for Health and Care Research (NIHR) Maudsley Biomedical Research Centre at South London and Maudsley NHS Foundation Trust and King's College London.

Contact: michelle.sader3@abdn.ac.uk

OT14

Calcified plaque imaging and detection in ex-vivo porcine heart arteries using a scalable, lead-free intravascular ultrasound array

Elmergue Germano[1,2*], Giulia Core[3], Ehsan Mohseni[1], David Lines[1], Kwok-Ho Lam[2], Joseph Kinney[2], David Russel[4], Jessie Gifford[5], Brian J. deGuzman, MD[5], David Hughes[3], Heather Trodden[3], Anthony Gachagan[1]

1. Centre for Ultrasonic Engineering, Department of Electronic and Electrical Engineering, University of Strathclyde, 16 Richmond St, Glasgow, G1 1XQ, UK
2. Centre for Medical and Industrial Ultrasonics, James Watt School of Engineering, University of Glasgow, University Avenue, Glasgow, G12 8QQ , UK
3. Novosound Ltd, Bo'Ness Rd, Motherwell, ML1 5UH, UK
4. School of Medicine, Dentistry & Nursing, Thomson Building, University of Glasgow, University Avenue, Glasgow, G12 8QQ , UK
5. PAVmed, 360 Madison Ave, Floor 25, New York, NY 10017,917-813-1828, United States

Keywords: Intravascular ultrasound (IVUS); Atherosclerosis; Coded excitation; Lead-free; Flexible ultrasonic array

Abstract:

Cardiovascular diseases are the leading cause of death worldwide, causing 17.9 million fatalities annually and posing social and economic burden. In Europe alone, they impose a €210 billion expense. Atherosclerosis, the accumulation of fats and other substances within arterial walls, leads to arterial narrowing, blocking blood flow. Percutaneous coronary interventions (PCI) are commonly used to restore arterial patency and optimise blood flow in coronary circulation. Intravascular ultrasound (IVUS) uses a catheter-mounted transducer to image vessel walls and atherosclerotic plaque, guiding PCI with notable advantages, including a 50% reduction in post-procedure cardiovascular mortality. Commercial IVUS catheters employ lead-based transducers, representing health and environmental risks. Transitioning to lead-free alternatives is crucial and timely to support global initiatives including the Restriction of Hazardous Substances (RoHS) regulation to advance environmentally sustainable piezoelectric technologies. Despite progress in understanding the piezoelectric properties of lead-free materials, scaling up their production remains challenging. A scalable, RoHS-compliant array transducer is presented. Coded excitation was employed to compensate the lower piezoelectric coefficient of the array relative to its lead-based counterparts, and demonstrate improved imaging and detection of calcified plaques in *ex-vivo* porcine heart arteries.

The 32-element array (163 µm-pitch, 3.82 mm-elevation, 5 French gauge) was characterised via electrical impedance and pulse-echo measurements. Coded excitation was used to address its signal-to-noise ratio challenge. The impedance magnitude showed uniformly damped responses, with the phase spectrum indicating resonance around 21 MHz. Pulse-echo analysis revealed a peak frequency at 19.22 ± 2.2 MHz, and a 66.80 % bandwidth (-6 dB). Comparative analysis including chirp, Barker and Golay excitations imaged the arterial wall, and B-scans across three samples detected calcified plaques. Subsequent investigations explored detection of dense fibrous plaques in arteries (down to approximately 8 mm diameter) using chirp. These findings highlight lead-free transducers as a sustainable, high-performance candidate for next-generation IVUS systems.

POSTER PRESENTATIONS

P000

Sound Stimulation for the Treatment of Alzheimer's Disease: Stimulus Optimisation

Idris Hallak [1], Keandra Suvarna[1], Toni Higgins[1], Amber Tan[1], Ajay McLaren[1], Tracy Silva[1], Hasan Saghari[1], James Dowsett[2], Ronan Breslin[3], Jessica Argo[3], Mario A. Parra[1], William J. McGeown[1]

1. Department of Psychological Sciences and Health, University of Strathclyde.
2. Department of Psychology, University of Stirling.
3. School of Innovation and Technology, The Glasgow School of Art.

Keywords: Clinical Applications, Cognitive Health, Auditory Intervention, 40 Hz Sound

Abstract:

Background:

Alzheimer's disease (AD) is a progressive neurodegenerative disorder with limited treatment options to slow disease progression. Notably, treatment/management of specific symptoms such as anxiety and agitation could also be improved. Recent research highlights the potential of 40Hz sound stimulation in modulating neural oscillations and reducing AD pathology, while environmental soundscapes (e.g., forest sounds) are known to promote relaxation and improve mood. However, the combined effects of 40Hz stimulation and soundscapes remain underexplored.

Aim:

This study aims to investigate how different volume levels of 40Hz sound stimulation, played in isolation and in combination with natural soundscapes, influence gamma frequency neural activity and subjective pleasantness and relaxation in healthy younger adults (before we later translate to older adults and patients with AD).

Methods:

Twenty-eight participants aged 17-30 will be recruited and exposed to five auditory conditions: 40Hz stimulation at low and medium volumes, soundscape alone, and combined 40Hz stimulation with soundscape (at both volume levels). Electroencephalography will be used to measure gamma power in the 40Hz range, and participants will provide subjective ratings of pleasantness and relaxation after each condition, followed by a semi-structured interview to further assess stimulus perceptions. We hypothesise that 1) the higher volume 40Hz stimulation will produce higher gamma neural power; 2) gamma neural entrainment will still be detectable when 40Hz flicker at either volume level is combined with the soundscape; 3) participants will report greater pleasantness and relaxation with soundscape-integrated conditions.

Discussion/Conclusions:

This study and the associated analyses will reveal the effects of 40Hz stimulation volume level on neural entrainment, and whether integrating 40Hz stimulation with natural soundscapes, can enhance participant comfort and still lead to gamma neural entrainment (indicating a potentially viable treatment option that will promote adherence). Further research in clinical populations is recommended to optimise sensory-based therapies for the treatment of AD.

Contact: abdelaziz.hallak.2024@uni.strath.ac.uk

P001

Radiogenomics Pilot Study: Correlating Radiomic Features with Single Nucleotide Polymorphism-Based Microarray Copy Number Variations for Classifying Benign Renal Oncocytoma and Chromophobe Renal Cell Carcinoma

Abeer Alhussaini[1,2,3,] Abirami Veluchamy[4], Adel Jawli [1,5], Neil Kernohan[6,] Benjie Tang [7], Colin N.A Palmer [8], J. Douglas Steele [1,2], Ghulam Nabi [1,9]

1. Division of Imaging Sciences and Technology, School of Medicine, Ninewells Hospital, University of Dundee, Dundee DD1 9SY, UK
2. Division of Neuroscience, School of Medicine, Ninewells Hospital, University of Dundee, Dundee DD1 9SY, UK
3. Department of Medical Imaging, Al-Amiri Hospital, Ministry of Health, Sulaibikhat, Kuwait City, Kuwait
4. Tayside Centre for Genomic Analysis, School of Medicine, University of Dundee, Dundee DD1 9SY, UK
5. Department of Clinical Radiology, Sheikh Jaber Al-Ahmad Al-Sabah Hospital, Ministry of Health, Sulaibikhat, Kuwait City, Kuwait
6. Department of Pathology, Ninewells Hospital, Dundee DD9 1SY, UK
7. Surgical Skills Centre, Dundee Institute for Healthcare Simulation Respiratory Medicine and Gastroenterology, School of Medicine, Ninewells Hospital and Medical School, University of Dundee, Dundee DD1 9SY, UK
8. Division of Population Pharmacogenetics, Population Health and Genomics, Biomedical Research Centre, Ninewells Hospital and Medical School, University of Dundee, Dundee DD1 9SY, UK
9. Division of Cancer Research, School of Medicine, Ninewells Hospital, University of Dundee, Dundee DD1 9SY, UK

Abstract:

Renal Oncocytoma (RO) and Chromophobe Renal Cell Carcinoma (ChRCC) are kidney tumours with overlapping characteristics, making their differentiation challenging. This study aims to develop a radiogenomics map by linking radiomic features to molecular phenotypes in ChRCC and RO, using resection as the gold standard. Fourteen patients (6 with RO and 8 with ChRCC) were included in this prospective study. A total of 1,875 radiomic features were extracted from CT scans, along with 632 cytobands encompassing 16,303 genes from genomic data. Feature selection algorithms identified 13 key radiomic features, while 24 cytobands highly correlated with histology were selected and cross-referenced with the radiomic data. The analysis revealed four radiomic features strongly associated with seven genomic features. These findings highlight the potential of integrating radiomic and genomic data to improve the differential diagnosis of RO and ChRCC, contributing to the development of more accurate and non-invasive diagnostic tools in clinical practice.

P002

Impact of Sleep Deprivation on Spatial Learning and Memory Performance in an Animal Model of Alzheimer's Disease

Hasan (Sina) Saghari [1]

1. Department of Psychological Science and Health, Faculty of Humanities and Social Science, University of Strathclyde, UK

Keywords: Sleep deprivation, Spatial Learning and Memory, Alzheimer's, Rat

Abstract:

One of the most prevalent forms of dementia is Alzheimer's disease (AD), characterized by progressive behavioral and cognitive impairments like sleep disturbances and memory loss. Studies suggest that there is a bidirectional relationship between sleep deprivation (SD) and AD pathology. This study aimed to investigate the effect of sleep deprivation on spatial learning and memory in an animal model of Alzheimer's disease. Forty-two rats were randomly assigned to six groups: vehicle, vehicle +large platform, vehicle +SD, Alzheimer, Alzheimer +large platform, Alzheimer +SD. AD was induced by the Amyloid-β (Aβ) 1-42 (5 mg/ml) peptide, which was administered bilaterally intracerebroventricular. The multiple platform method was used to induce sleep deprivation. Spatial learning and memory performance were evaluated by the Morris Water Maze (MWM) test. Our results indicate that sleep deprivation significantly exacerbated spatial learning and memory impairments in rats with AD.

Acknowledgements:
This work was supported by the Neuroscience Research Center of Kerman Medical Science University, Iran.

Contact: hasan.saghari@strath.ac.uk

P003

Synthetic High-Quality Computed Tomography (CT) Image Generation from Low-Quality Cone-Beam CT

Alzahra Altalib[1], Chunhui Li[1], Alessandro Perelli[1]

1. School of Science and Engineering University of Dundee, UK

Keywords: synthetic CT, CBCT, radiotherapy planning, dose calculation, deep learning

Abstract:

Cancer is a complex and potentially fatal disease that requires advanced treatment strategies to manage its progression. Radiotherapy, a key treatment modality, employs high-energy radiation to target and destroy cancerous tumours. To optimize the precision of radiation delivery while minimizing damage to surrounding healthy tissues, radiotherapy treatment planning is essential. Recent advancements such as 3D conformal radiotherapy and image-guided radiation therapy have enabled the personalization of treatment to align with patients' unique anatomies. Nevertheless, irregular tumour shapes pose challenges in achieving uniform dose distributions, often leading to incidental exposure of adjacent critical organs [1]. To address these challenges, advanced computing methods—including deep learning and model-based learning—are increasingly integrated into radiotherapy workflows. These techniques typically rely on standard imaging modalities like Computed Tomography (CT), which provides the high-resolution anatomical detail necessary for accurate patient positioning. However, repeated CT scans can result in elevated radiation doses.

Cone-Beam Computed Tomography (CBCT) offers a promising alternative by enabling rapid 3D image acquisition with reduced radiation exposure, thereby enhancing patient comfort. Yet, CBCT images are often compromised by artefacts, poor soft tissue contrast, and geometric distortions, which limit their utility in precise dose estimations. The aim of this research is to synthesize high-quality CT images from low-dose CBCT data using deep learning, thereby enabling accurate radiation dose calculations during radiotherapy planning while reducing overall radiation exposure.

The study proposes a novel deep-learning framework to generate synthetic CT images from CBCT scans. Phantom studies mimicking human tissue and tumour properties will be conducted to validate the approach. Synthetic images will be compared against high-quality CT scans acquired under identical conditions to assess fidelity. Subsequently, dose calculations based on the synthetic CT images will be benchmarked against those derived from the reference CT scans. If dose deviations fall within clinically acceptable thresholds, this approach could significantly reduce patient radiation exposure without compromising treatment accuracy. Figure 1 illustrates the image synthesis and dose estimation workflow.

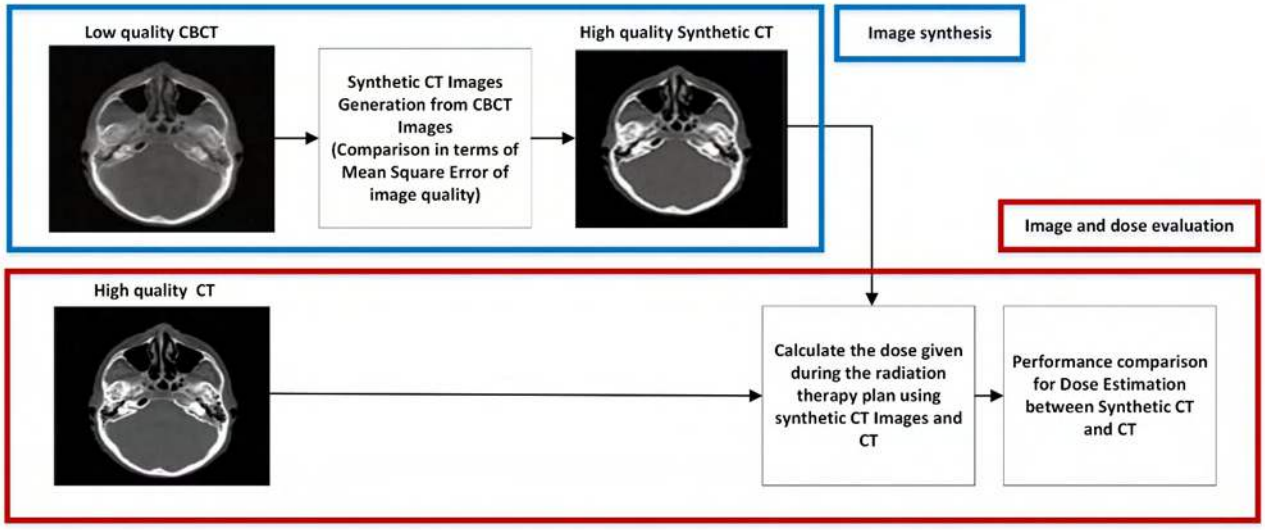

Figure 1: Synthetic CT Images Generation and Dose Estimation using CBCT data
CT and CBCT Scans Source. Adapted with permission from [2].

References:

[1]. Nuyts, S. (2007). Defining the target for radiotherapy of head and neck cancer. Cancer Imaging, 7(Special issue A), S50–S55. https://doi.org/10.1102/1470-7330.2007.9009

[2]. Thummerer, A., Zaffino, P., Meijers, A., Marmitt, G. G., Seco, J., Steenbakkers, R. J., ... & Knopf, A. C. (2020). Comparison of CBCT based synthetic CT methods suitable for proton dose calculations in adaptive proton therapy.

Contact: 12600129@dundee.ac.uk, aperelli001@dundee.ac.uk, c.li@dundee.ac.uk

P004

Sexual dimorphism in resting state functional connectivity - an exploratory study of 1043 subjects

Anca-Larisa Sandu[1], Tina Habota[1], Chris McNeil[1], Gordon D Waiter[1], Andrew M McIntosh[2], Heather Whalley[2], Alison D Murray[1]

1. Aberdeen Biomedical Imaging Centre, University of Aberdeen
2. Centre for Clinical Brain Sciences, University of Edinburgh

Keywords: Image analysis, Psychology/Psychiatry (Cognitive Neuroimaging)

Abstract:

Introduction:

Brain functional connectivity shows a sexual dimorphism. For example, Jadamar et al. showed that males have greater connectivity than females in the salience network. Females showed greater connectivity than males in the default mode network. The current study analyses sex differences in functional connectivity in a larger data set and using different atlases.

Method:

Under the umbrella of Stratifying Resilience & Depression Longitudinally (STRADL) study, 1043 participants from Aberdeen and Dundee had resting state fMRI acquired. MRI included a volumetric scan (TR/TE=8.3/3.8ms; Matrix= 240x240; n slices=160; thickness=1mm) and resting state fMRI (TR=1560ms, TE=26ms, 32 transverse slices, matrix=64x64, pixel size=3.39 x 3.39mm2, slice thickness=4.5mm, volumes=195). Data were analysed using the functional connectivity toolbox CONN (https://www.nitrc.org/projects/conn).
From those 1043 participants 59% are women and 41% are men (age range 27- 85 years).
Functional connectivity ROI-to-ROI analyses were used to determine the brain connections in women and in men. The target ROIs were selected from the FSL Harvard Oxford and AAL (cerebellar areas only) atlases.

Results:

The model includes the age of participants as a covariate and between-subject contrast, females and males. Difference with an FDR-corrected $p<.05$ were considered statistically significant.
The connections between Precuneus and Middle Temporal Gyrus (MTG) and also connections from amygdala and hippocampus to MTG are stronger in women than in men. Similarly, Weis et al. (2020) found stronger connection in limbic system for women.
All the differences are summarized in Figure 1.
Data show correlations between sex and regionally specific brain connectivity, however they do not support a clear-cut dimorphism in functional brain organization that is driven by sex and age alone.

References:

[1] Jadamar et al. Sexual Dimorphism of Resting-State Network Connectivity in Healthy Ageing. Cognitive Neuroscience of Aging. *J Gerontol B Psychol Sci Soc Sci*, 2019, Vol. 74, No. 7, 1121–1131.
[2] Susanne Weis et al. Sex Classification by Resting State Brain Connectivity *Cerebral Cortex,* February 2020;30: 824–835

Acknowledgements:

The authors would like to thank to the participants from Aberdeen and Dundee for their voluntary contribution to the STRADL project (Stratifying Resilience & Depression Longitudinally). The present study is funded by Wellcome Trust Strategic Award (Ref: 104036/Z/14/Z) to AMM and a Roland Sutton Academic Trust project (Ref: 0066/R/19) to ALS.

Contact: anca.sandu-giuraniuc@abdn.ac.uk

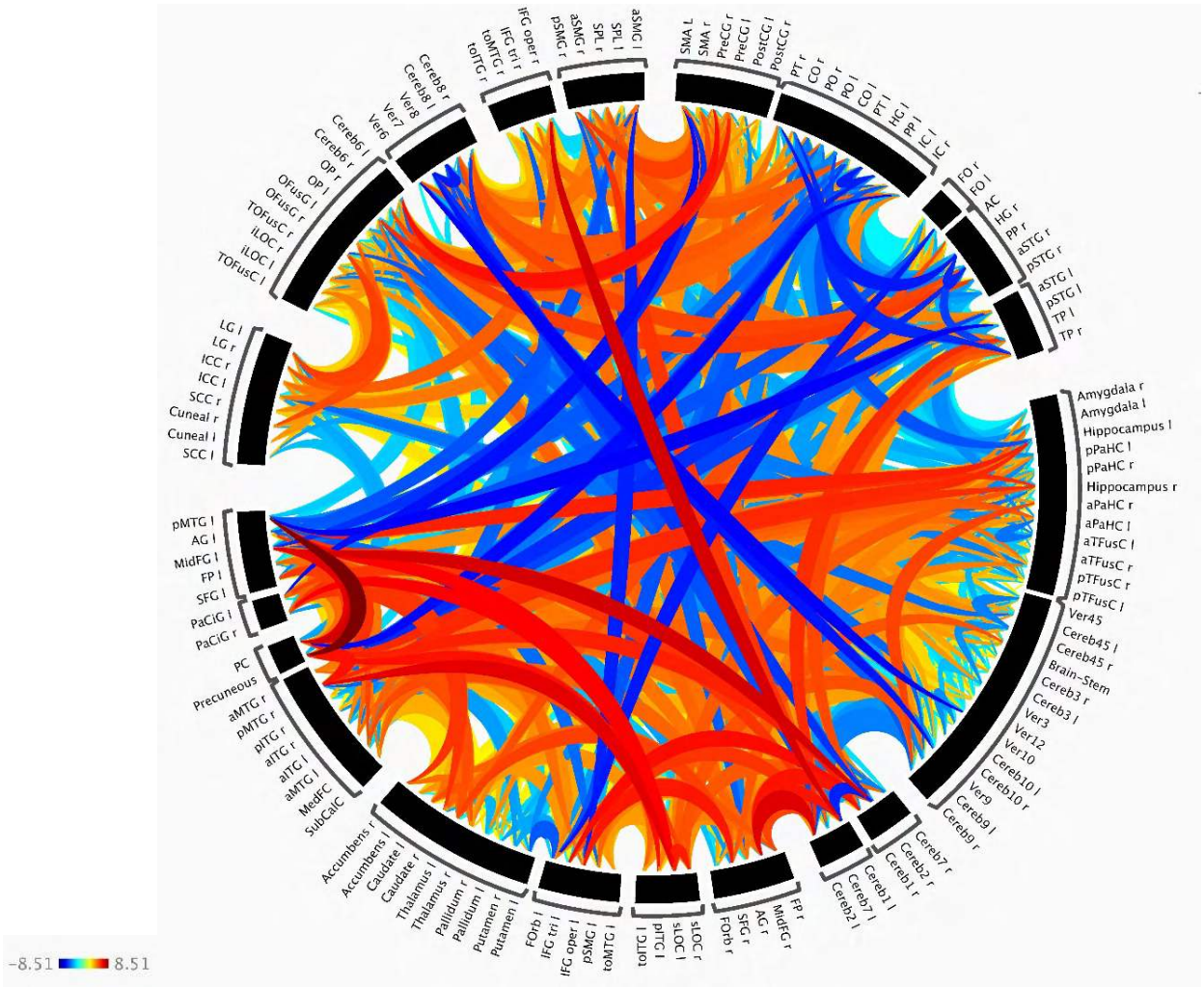

Figure 1 The connectome for resting state functional connectivity described by the difference between women and men. Red – positive correlations, blue – negative correlations.

P005

Influence of winter and summer seasons on hippocampal and hippocampal subfield volumes – using longitudinal magnetic resonance imaging volumetric data

Filip Skoczylas[1], Gordon Waiter[2]

1. NHS Grampian, Radiology Department
2. School of Medicine, Medical Sciences and Nutrition

Relevant Keywords: Hippocampus, photoperiod, volume, subfields

Abstract:

Background:

The hippocampus plays a vital role in memory, and its structure may be influenced by seasonal variations in photoperiod. This study investigates whether hippocampal volumes change across seasons, specifically comparing measurements between summer and winter.

Objective:

The aim is to examine the effects of seasonal daylight exposure on hippocampal volume in healthy individuals, hypothesizing that volume differences will correlate with changes in photoperiod.

Methods:

Fifteen healthy subjects underwent T1-weighted MRI scans twice, in June and December 2022. Hippocampal subfields' volumes were measured using FreeSurfer software, adjusting for total intracranial volume and total brain volume in order to control for subject size and background age-related brain atrophy.

Results:

Significant volume changes were observed, with increases in the left molecular layer HP head (5.59%), left whole hippocampal body (1.13%), and left whole hippocampus (0.89%) from June to December. Conversely, the right CA3-head exhibited a decrease of 3.29%. These findings suggest that some hippocampal regions enlarged during winter, contrary to established literature linking longer daylight exposure with increased volumes.

Conclusion:

This study presents mixed results regarding the influence of photoperiod on hippocampal subfield. Including contradictory findings showing increase overall hippocampal volume during winter periods. Most subfields did not show significant change, but some subfields, depending on laterality showed increased volumes whilst others showed decreased volumes. Further research is necessary to clarify these findings and explore their implications for conditions where the hippocampus and photoperiod is implicated in their pathophysiology such as dementia and seasonal affective disorder.

Contact: filip.skoczylas@gmail.com

P006

Can Artificial Intelligence (AI) Techniques Improve the Detection of Lung Cancer in PET/CT Imaging? A Systematic Review and Meta-Analysis.

Fahad Alkhaldi[1]. Meshaal Alenezi[2]. Andy Welch[3]. Noor Almualim[4]. Sultan Alkhaldi[5]. Salem Alanazi[6]. Maryam Alhashim[7]. Mohamed Yousef[8]. Salihah Alhamami[9]. **Wafaa Alghamdi[3]**

1. Department of Radiology, Ministry of National Guard Health Affairs, Riyadh, Saudi Arabia.
2. King Khalid Hospital, Hail Health Cluster, Ministry of Health, Hail, Saudi Arabia.
3. Faculty of Biomedical Sciences, University of Aberdeen, Aberdeen, UK.
4. Department of Radiology, Alzahra General Hospital, Eastern Province, Saudi Arabia.
5. Department of Radiology, Ministry of National Guard Health Affairs, Taif, Saudi Arabia.
6. Medical Cities Program, General Directorate of Medical Services, Ministry of Interior, Riyadh, Saudi Arabia.
7. Department of Radiology, College of Medicine, Imam Abdulrahman bin Faisal University, Dammam, Saudi Arabia.
8. Radiological Science Program, Batterjee Medical College, Jeddah, Saudi Arabia
9. Department of Radiology, Najran University Hospital, Najran, Saudi Arabia.

Keywords: lung cancer, artificial intelligence, PET/CT, clinical applications, image analysis.

Abstract:

Background: Lung cancer accounts for the majority of cancer-related deaths worldwide. Early diagnosis and preventive interventions are critical for improving survival rates. However, manual diagnosis is time-consuming and burdensome for radiologists. As artificial intelligence (AI) models evolve, their use in biomedical image analysis for disease detection—especially cancer—has gained attention. Despite promising efforts, challenges remain in achieving high diagnostic accuracy and clinical acceptance.

Aims: This systematic review aimed to evaluate the diagnostic accuracy of AI models in detecting lung cancer using PET/CT imaging. Although AI has been explored in many medical domains, its specific performance in PET/CT-based lung cancer detection remains under-investigated.

Methods: A systematic search was conducted across medical databases to identify studies developing or evaluating AI models for lung cancer detection via PET/CT. After screening and full-text review, ten eligible studies (six deep learning [DL] and four machine learning [ML]) were selected. These models were assessed and pooled for a quantitative synthesis.

Results: Data from six DL studies involving 844 participants showed a pooled sensitivity of 91.3% (95% CI: 86.5%–95.9%). Four ML studies covering 710 samples reported an overall sensitivity of 87.5% (95% CI: 79.6%–95.5%). These findings indicate robust diagnostic performance across both model types.

Conclusion: The reviewed studies demonstrate promising sensitivity and accuracy in distinguishing lung malignancies through AI-based PET/CT analysis. Many AI models outperformed manual diagnosis in key performance metrics. However, further validation in larger, more diverse populations is essential to confirm reliability and reduce potential biases. The evidence suggests that ML and DL tools are likely to play a substantial role in the future of AI-driven lung cancer screening.

Contact: Fahadalkhaldi277@gmail.com

P007

Incorporating Visual Surgical Tool Priors into Language Models for Semantic Keypoint Estimation

Krit Duangprom, Tryphon Lambro, Binod Bhattarai

1. School of Natural and Computing Sciences, Computing Sciences, University of Aberdeen, UK

Keywords: keypoint estimation, Surgical tool estimation, hand estimation, vision-language models, large language model

Abstract:

Precise understanding of surgical tool and hand positioning is essential for advancing training, enhancing procedural accuracy, and supporting medical operations. Recent advances in large language models (LLMs) have demonstrated their ability to encode semantic knowledge through extensive pretraining, presenting new opportunities for enhancing keypoint detection and generalization in complex, domain-specific tasks such as surgical tool and hand analysis. However, keypoint estimation in surgical settings presents unique challenges — unlike human pose estimation, surgical instruments often lack standardized or semantically defined keypoints, making annotation task-specific and ambiguous. In this work, we propose a vision-language framework for estimating semantic 2D keypoints of surgical tools and hands from RGB images. Our method leverages a visual encoder pre-trained with surgical tool priors, enabling it to focus on anatomically and functionally relevant tool regions. These features are then interpreted by a language model guided by domain-specific prompts. We fine-tune the model using a set of keypoints defined by the semantics of tools and hand. A low-rank adaptation strategy is used to incorporate this contextual pose information efficiently, without requiring full model retraining. Our current focus is on accurate 2D keypoint localization, the framework can be extended to 6D pose estimation. We compare our method against conventional models that do not incorporate language understanding, in order to evaluate differences in accuracy, adaptability, and interpretability. This modular, language-informed method may support new forms of interactive surgical guidance and skill assessment tools.

Acknowledgements

Contact: r01kd24@abdn.ac.uk

Model	Mean Per Joint Position Error (MPJPE)
Yolov8	130
Yolov8 + Transformer module	119
Our	112

Figure 1. *Comparison of Mean Per Joint Position Error (MPJPE) between our method and models without language integration*

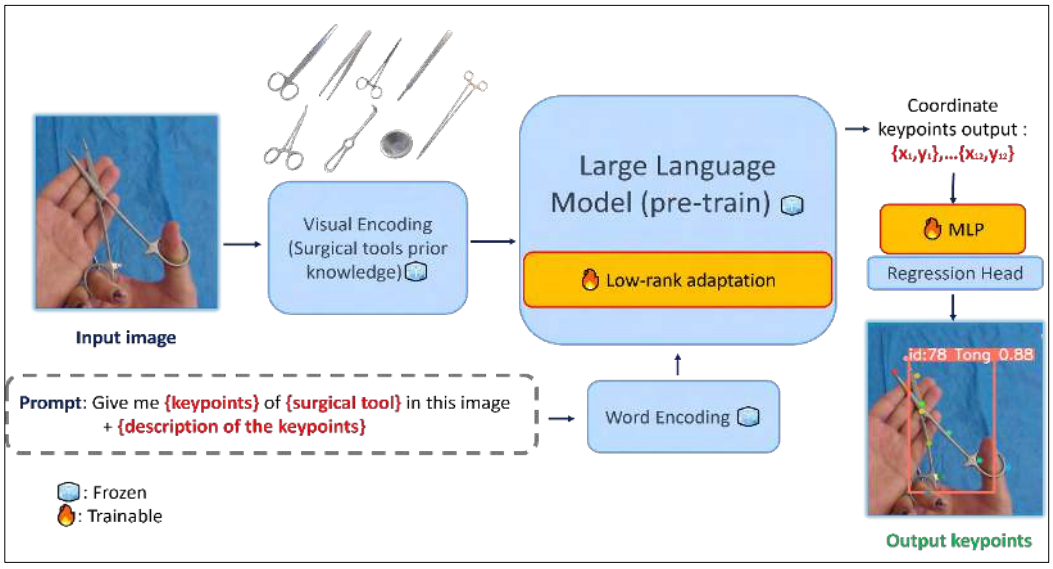

Figure 2. *Overview of the proposed framework. An input image and text prompt are processed by a pretrained visual encoder and large language model. Using low-rank adaptation for efficient fine-tuning, the fused features are passed through an MLP and regression head to predict semantic 2D keypoints.*

P008

Large volume of magnetic-resonance imaging (MRI)-visible perivascular spaces associate with impaired cognition and cognitive decline. A multicentre individual patient data meta-analysis

Francesca Chappell[1], Roberto Duarte Coello[1], **Maria del C. Valdés Hernández[1]**, Rosalind Brown[1], José Bernal Moyano[1,2], Lucia Ballerini[1], Joel Ramírez[3], Stephanie Berberian[3], Hugo Kuijf[4], Alberto De Luca[4], Geert Jan Biessels[4], Sandra Black[3], Joanna M. Wardlaw[1]

1. Centre for Clinical Brain Sciences, University of Edinburgh, Edinburgh, UK
2. DZNE Magdeburg, Germany
3. University of Toronto, Canada
4. UMC Utrecht Brain Center, UMC Utrecht, The Netherlands

Keywords: image analysis, brain MRI, perivascular spaces, cognition, meta-analysis

Abstract:

Introduction:

Perivascular spaces (PVS), when enlarged, can be quantified from brain magnetic resonance images (MRI). They have been associated with increasing age, hypertension, sleep problems, and are a marker of small vessel disease, but their association with cognition in adults is unclear.

Methods:

We segmented MRI-visible PVS in MRI and used cognitive data acquired retrospectively from 14 studies of ageing, dementia, and vascular disease. We counted the number of PVS and quantified their volume separately in the basal ganglia (BG) and cerebral white matter mainly including the centrum semiovale (CSO). We converted general cognitive scores (i.e., MoCA and TorCA) into a percentage of the maximum score and conducted two meta-analysis: cross-sectional using a linear mixed model, and longitudinal using logistic regression to evaluate prediction of being cognitively normal or developing a cognitive impairment. Study was a random effect for both models.

Results:

The meta-analysis comprised 17771 participants. The percentage of PVS volume in the region of interests had a consistent negative relationship with cognition in cross-sectional analyses across different studies whether adjusted or not for various other known predictors of cognitive decline such as white matter hyperintensities (a common feature of vascular damage) and years of education. A 10% change in CSO PVS volume would estimate a 2% reduction in cognitive score. Longitudinally, in 2447 participants from 11 studies, larger normalised PVS volumes tended to predict a greater likelihood of any cognitive impairment, although this relationship may vary according to the participant populations (healthy aging, stroke, memory clinic) and/or other long-term brain changes (e.g. atrophy, worsening WMH), or variation in duration of follow-up.

Conclusions:

The volume of MRI-visible PVS impact ageing, vascular or neurogenerative processes leading to cognitive decline. More longitudinal data are needed to confirm the association. Other PVS measures may be more sensitive to cognitive decline.

Acknowledgements:
This work is supported primarily by The Galen and Hilary Weston Foundation under the Novel Biomarkers 2019 scheme (ref UB190097) administered by the Weston Brain Institute.

Contact: M.Valdes-Hernan@ed.ac.uk

P009

The Effects of Sex and Optic Neuritis on the Retina—Brain Connection in Adults with Relapsing-Remitting MS

Miracle Ozzoude[1,2,3], Rozanna Meijboom[2,3,4], Jamie Burke[1,3,5], Niall J. J. MacDougall[6], Elizabeth N. York[2,3,4], Charlene Hamid[3], Michael J. Thrippleton[2,3], Baljean Dhillon[1,2,7], Adam D. Waldman[2,3,4], Siddharthan Chandran[2,4], and Tom J. MacGillivray[1,2,3] on behalf of the FutureMS Consortium

1. Curle Ophthalmology Suite, Institute for Regeneration and Repair, University of Edinburgh, Edinburgh, UK
2. Centre for Clinical Brain Sciences, University of Edinburgh, Edinburgh, UK
3. Edinburgh Imaging, University of Edinburgh, Edinburgh, UK
4. Anne Rowling Regenerative Neurology Clinic, University of Edinburgh, Edinburgh, UK
5. School of Mathematics, University of Edinburgh, UK
6. Department of Neurology, Institute of Neurological Sciences, Queen Elizabeth University Hospital, Glasgow, UK
7. Princess Alexandra Eye Pavilion, NHS Lothian, Edinburgh, UK

Keywords: Optic neuritis, Multiple sclerosis, Optical coherence tomography, Magnetic resonance imaging, Sex-related differences

Abstract:

Introduction:
Sex differences may influence MS pathophysiology; while females have a higher MS risk, males often experience worse progression. Trans-synaptic degeneration (TSD), triggered by optic neuritis (ON) or brain inflammation, may drive widespread neurodegeneration, which may contribute to long-term disability**.** Whether TSD differs between sexes in relapsing-remitting MS (RRMS) following ON remains unclear.

Objectives/Aims:
To investigate sex-related differences in TSD in early-stage RRMS.

Methods:
People recently diagnosed (<6 months prior to baseline) with RRMS were recruited to FutureMS, a Scottish multi-centre longitudinal cohort study. Cross-sectional 3T magnetic resonance imaging and optical coherence tomography were used. Thalamic volume was segmented with FreeSurfer-v6; Peripapillary retinal nerve fibre layer (pRNFL) and ganglion cell–inner plexiform layer (GCIPL) metrics were extracted using OCTolyzer software. Expanded Disability Status Scale (EDSS) was performed on all participants. Sex-related comparisons were performed separately for ON and non-ON groups using t-tests or Mann-Whitney U-tests. Generalised estimating equations assessed sex and ON effects on retina-brain associations, adjusted for age and imaging site, and multiple comparisons corrected.

Results:
Data from 161 participants (120 Female: mean age ± SD yrs: 37.4±9.7; median EDSS: 2.0; 41 Male: mean age ± SD yrs: 36.2±11.5; median EDSS: 2.5) were analysed. ON history was more common in males (39%) than females (34%) ($\chi^2(1)=33.5$, $p<0.01$). In the ON group, males had significantly lower pRNFL thickness (temporal, superior-temporal), GCIPL thickness and volume (nasal), and thalamic volume (p.adjust<0.05). Lower thalamic volume was associated with lower nasal GCIPL measures in Males-ON than Females-ON (p.adjust<0.05) (Fig. 1). No sex differences were found in the non-ON group.

Conclusion: Males with RRMS may experience more severe TSD post-ON than females, with no sex differences in non-ON participants. Findings may support GCIPL and thalamic metrics as TSD markers and suggest greater visual pathway vulnerability in Males-ON. Longitudinal analyses will assess progression of sex-related TSD in MS.

Acknowledgements:
We would like to thank all non-author contributors of the FutureMS consortium. With special thanks to all FutureMS participants who have made this study possible.

Funding:
FutureMS was hosted by Precision Medicine Scotland Innovation Centre (PMS-IC) and funded by a grant from the Scottish Funding Council to PMS-IC and Biogen Idec Ltd Insurance (combined funding under reference Exemplar SMS_IC010). Additional support for authors came from Medical Research Council (MRC-UK) Doctoral Training Partnership (DTP) in Precision Medicine (M.O); MS Society UK Centre of Excellence (UK), Anne Rowling Regenerative Neurology Clinic (UK), and Chief Scientist Office Scotland (UK) (R.M); and MS Society UK Centre of Excellence (UK) (E. N. Y.).

Contact: m.e.ozzoude@sms.ed.ac.uk

P010

Impact of Anthocyanins on Resting-State fMRI Functional Networks in a Prodromal Dementia Population

Oystein Kallevag[1,2,3,4], Khadija Khalifa[2], Dag Aarsland[2,5]

1. Stavanger Medical Imaging Laboratory (SMIL), Radiology department, Stavanger University Hospital, Stavanger, Norway
2. Centre for Age-Related Medicine (SESAM), Stavanger University Hospital, Stavanger, Norway
3. University of Stavanger, Faculty of Science and Technology, Stavanger, Norway
4. Aberdeen Biomedical Imaging Centre, University of Aberdeen, Aberdeen, UK
5. Centre for Healthy Brain Ageing, Institute of Psychiatry, Psychology, and Neuroscience, King's College London, London, UK

Keywords: dementia, cognition, image analysis, fMRI, anthocyanins.

Abstract:

Background:
Anthocyanins, found in dark berries and fruits, are among the dietary factors that may help ameliorate age-related cognitive decline. Observations have suggested antioxidant and anti-inflammatory effects in the brain, and anthocyanins may enhance cognitive function and lower the risk of dementia development. In this study, we investigated whether functional connectivity measured with resting-state fMRI could show treatment effects not found with traditional cognitive tests.

Method:
From 2018 to 2020, we performed a 24-week randomized, double-blind, placebo-controlled study on cognitively healthy individuals, defined by the Mini-Mental State Exam (MMSE) and Clinical Dementia Rating (CDR). Anthocyanins were administered in Medox® capsules containing 80 mg of natural purified anthocyanins, with a dosage of 4 capsules daily (i.e., 320 mg/day of anthocyanins). 86 participants completed the resting-state fMRI (rsfMRI) examination at baseline and week 24 using a Philips Ingenia 3.0T scanner at Stavanger University Hospital. Functional images were preprocessed, denoised, and analyzed using the default options in CONN22.v2407. Cognitive testing was performed using CogTrack®, an online digital cognitive test battery.

Result:
The mean age of the participants was 69.15 (± 5.65) years, and the mean MMSE score was 28.94 (± 1.30). The functional connectivity analysis did not reveal any significant differences in connectivity between baseline and week 24 for the intervention group.

Conclusion:
Our results show no significant differences in connectivity measures after 24 weeks of intervention with anthocyanins. This suggests that rsfMRI and cognitive tests do not provide evidence for any treatment effect over a period of 24 weeks in a population of older adults at risk of developing dementia.

Contact: oystein.kallevag@sus.no

P011

Mitigating transmit magnetic field inhomogeneity using a neurovascular head and neck coil with tailored parallel transmission pulses

Chia-Yin Wu[1*], Divya Baskaran[1], Keith Muir[1], Natasha Eileen Fullerton[1,2], Shajan Gunamony[1,3], David Andrew Porter[1]

1. Imaging Centre of Excellence, University of Glasgow, Glasgow, UK
2. Department of Neuroradiology, Institute of Neuroscience, NHS Greater Glasgow and Clyde, Glasgow, UK
3. MR CoilTech Limited, Glasgow, UK

Keywords: head and neck, **parallel transmission, ultra-high field**

Abstract:

Introduction:

A 7T neurovascular head-and-neck coil (NVHN)[1] provides coverage of the brain and cervical spine regions enabling various neurovascular imaging techniques at ultra-high field (UHF). UHF systems significantly improve SNR and parallel-imaging but capabilities are challenged by non-uniform transmit magnetic fields (B_1^+). Parallel transmission (pTx) can be used to mitigate the B_1^+ problem[2]. With a single dedicated NVHN coil (Fig.1), tailored pTx pulse designs can remain more streamlined without the need of coordinating multiple coils imaging different anatomical regions. Here we demonstrate an initial phantom evaluation using a NVHN coil with tailored pTx pulses to improve signal uniformity across the brain and neck region.

Methods:

All data were collected on a 7T Terra system (Siemens, Germany) using a custom-built 8TxRx56Rx NVHN coil. Absolute and relative B_1^+ maps were acquired using a phantom to design tailored pTx pulses. Non-selective tailored pTx pulses (8 k_T-points[2]) were designed using the MLS spatial-domain-method[3,4]. 3D GRE datasets were acquired with 5° and 9° flip-angle pulses. Acquisitions were made using the standard non-selective excitation pulse in the circularly polarised (CP) mode and with pTx pulses. Combined with the SA2RAGE[5] maps, the ratio between the CP and pTx images was used to construct flip-angle maps produced by each pulse.

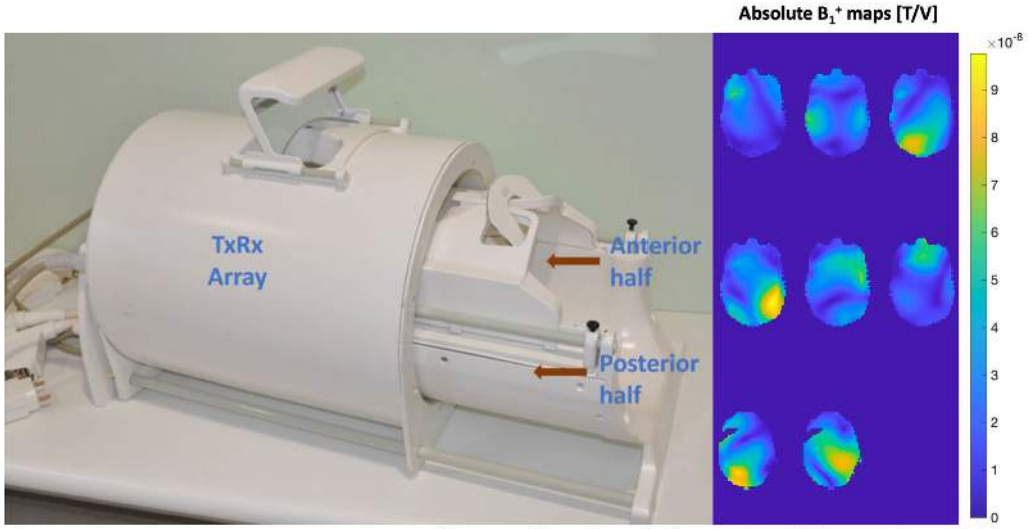

Figure 1. *Left: 8TxRx56Rx Neurovascular Head-and-Neck (NVHN) coil (Image from [1]). Right: Transmit sensitivity maps measured for each of the 8Tx-channels.*

Results:

As shown in Figure 2, significant improvements in excitation fidelity was achieved in the peripheral regions of the head extending down to the upper neck region in pTx-mode. The pTx pulses produced superior excitation uniformity with a NRMSE of 0.20 in comparison to 0.33 using CP-mode for 5° flip-angle. Similarly, a NRMSE of 0.19 was achieved for 9° flip-angle using pTx.

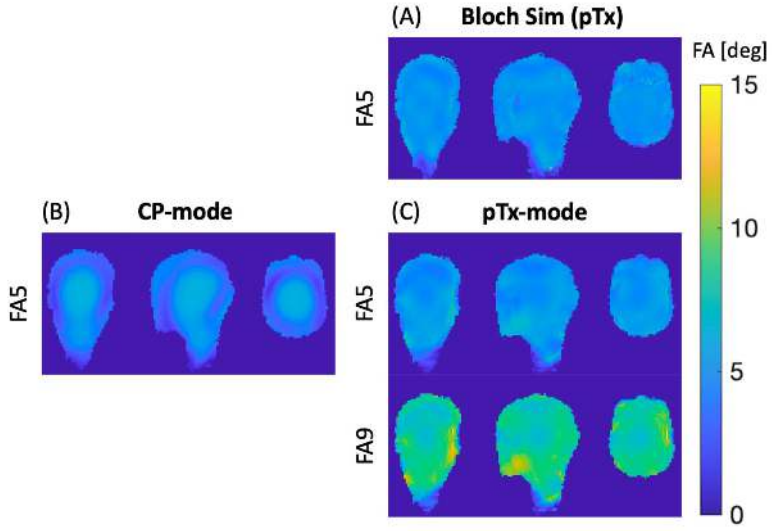

Figure 2. *(A) Simulation of the tailored pTx pulse with 5° flip-angle. Measured flip-angle maps using (B) CP-mode with and (C) pTx-mode with 5° and 9° flip-angles.*

Conclusion:

Tailored pTx pulses can improve excitation fidelity across both brain and neck regions. The next step is to evaluate the feasibility in vivo.

Acknowledgements:

This project is funded by Scottish Funding Council, grant H07012/242700324, the Christine Rodgers endowment fund, the Neuroscience Foundation, the Strength in Places fund, and Innovate UK through The Living Laboratory: driving economic growth in Glasgow through real world implementation of precision medicine (award Ref: 107140). The authors also thank Robin Sayer and Iain Hendry from the NHS Medical Devices Unit for providing the mechanical design for this coil.

References:

1] Baskaran et al. MRM. 2024. 2] Cloos et al. MRM. 2012. 3] Grissom et al. MRM. 2006. 4] Setsompop et al. MRM. 2008. 5] Eggenschwiler et al. MRM 2012.

Contact: chia-yin.wu@glasgow.ac.uk

P012

T1 rho MRI for Takotsubo Cardiomyopathy

Liene Balode[1*], Robert Kelly[2], David Gamble[2], Dana Dawson[2], P. James Ross[1]

1. Aberdeen Biomedical Imaging Centre, University of Aberdeen, UK
2. Aberdeen Cardiovascular and Diabetes Centre, University of Aberdeen, UK

Relevant Keywords: Quantitative MRI, T1 rho, Takotsubo Cardiomyopathy

Abstract:

Introduction:

In addition to conventional parametric mapping that use the spin-lattice (T1) and spin-spin (T2) relaxation mechanisms, a new native image parametric mapping method using spin-lattice relaxation in the rotating frame (T1 rho) has been recently described. T1 rho relaxation is sensitive to the low-frequency (Hz-kHz) ^{1}H motion; therefore, it can be used to investigate the exchange of protons between water and macromolecules [1]. We aimed to investigate the use of T1 rho MRI for detecting myocardial changes in acute takotsubo cardiomyopathy patients. Takotsubo cardiomyopathy is a temporary and severe left ventricular dysfunction caused by extreme emotional or physical stress [2], that confers significant mortality and morbidity.

Methods:

After informed consent, takotsubo cardiomyopathy patients (n=51) and healthy volunteers (n=16) were scanned using a 3.0 T MRI scanner (Achieva dStream, Philips, Amsterdam, Netherlands). An electrocardiogram (ECG) triggered imaging sequence starts with a spin-lock (SL) pulse (90x-SLy-180y-SL-y-90-x) which is followed by a breath-held single-shot balanced steady-state free precession (bSSFP) image acquisition. Takotsubo cardiomyopathy patients had a follow up scan after 12 weeks. The quantitative analysis of the T1 rho maps was performed using the Philips IntelliSpace Portal software.

Results:

The quantitative analysis of T1 rho maps showed that compared to healthy controls, in takotsubo cardiomyopathy patients, there was a significant increase in T1 rho during acute presentation, which improved at 12 weeks from baseline but remained significantly increased at both mid-cavity and apical levels of the left ventricle (Figure 1).

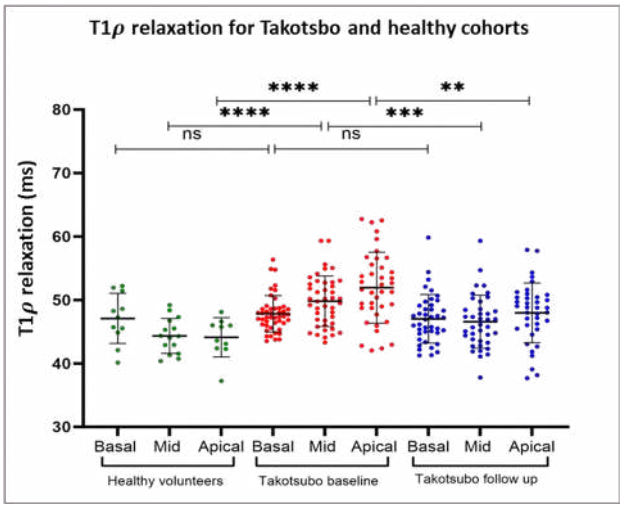

Figure 1. T1 rho relaxation measurements of basal, mid and apical segments from Takotsubo and healthy volunteer cohorts. Not significant (ns), $P > 0.05$, * $P \leq 0.05$, ** $P \leq 0.01$, *** $P \leq 0.001$, **** $P \leq 0.0001$.

Discussion

T1 rho MRI has shown potential for the detection of takotsubo cardiomyopathy in the acute phase.

References

[1] Wang P, Block J, Gore JC. Chemical exchange in knee cartilage assessed by R1ρ (1/T1ρ) dispersion at 3T. Magn Reson Imaging. 2015;33(1):38-42

[2] Singh T, Khan H, Gamble DT, Scally C, Newby DE, Dawson D. Takotsubo Syndrome: Pathophysiology, Emerging Concepts, and Clinical Implications [published correction appears in Circulation. 2022 May 17;145(20): e1053

Contact: l.balode.22@abdn.ac.uk

P013

Deep-learning Enhanced Cerebral Blood Flow Monitoring with SPAD Diffuse Correlation Spectroscopy

Mingliang Pan[1*], Chenxu Li, Yuanzhe Zhang, Quan Wang, David Li[1]

1. Department of Biomedical Engineering, University of Strathclyde, UK

Relevant Keywords: diffuse correlation spectroscopy, SPAD, deep learning, cerebral blood flow measurement

Abstract:
Diffuse correlation spectroscopy (DCS) analyzes the autocorrelation function of photons scattered by red blood cells, enabling non-invasive, continuous measurement of deep tissue blood flow at the bedside. Multi-layer DCS models (two- and three-layer) enhance cerebral blood flow index (CBFi) sensitivity and mitigate interference from extracerebral tissues. However, these models require multiple predefined parameters and are computationally intensive, making them impractical for real-time bedside monitoring. To address this challenge, we integrate a single-photon avalanche diode (SPAD) array with a deep learning (DL)-based approach trained on data generated by the two-layer analytical model. This method bypasses traditional model fitting, enabling real-time CBFi monitoring while minimizing superficial tissue contamination. We first validate our approach using Monte Carlo-simulated test datasets, demonstrating superior accuracy in relative CBFi estimation (5.8% error vs. 19.1% for conventional fitting) and enhanced CBFi sensitivity (87.1% vs. 55.4%).

Additionally, our method effectively isolates shallow blood flow changes and is 750-fold faster than single-exponential fitting in a realistic scenario. We further evaluate the system in a healthy adult, achieving real-time CBFi monitoring and pulsatile waveform recovery during a brain activity test using a 512×512 SPAD array sensor. These results highlight the potential of our approach for real-time brain activity monitoring.

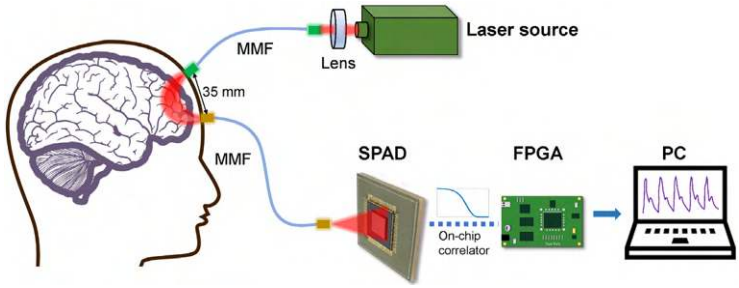

Figure 1. The SPAD-DCS system setup. The 785 nm continuous wave laser was coupled into a multi-mode fiber (MMF, M143L01, Ø600 μm, 0.22 NA, Thorlabs), the scattered photons was collected by another MMF (M59L01, Ø1000 μm, 0.50 NA, Thorlabs). The output of the SPAD array was received by an Opal Kelly FPGA board (XEM7310-A200) and transferred to the PC through a USB 3.0 cable. The on-chip computed ACF is sent to the trained DL model for real-time CBFi/rCBFi display.

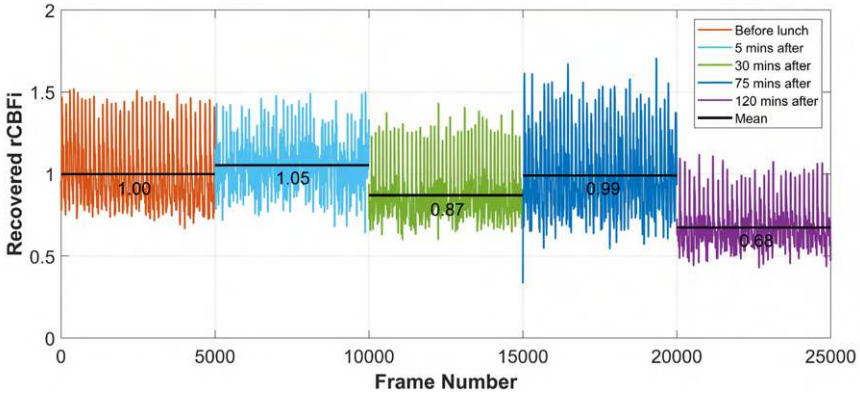

Figure 2. Cerebral perfusion monitoring using the proposed DL model during a simple brain activation paradigm (eating lunch, male, 29-year old). CBFi measurements were taken 30 minutes before and 5, 30, 75, and 120 minutes post-meal to assess digestion-induced cerebral perfusion changes. In each test phase, 5000 frames of autocorrelation data were collected using our SPAD-DCS system (Figure 1). The black lines represent the mean values of the recovered rCBFi at each test phase. The mean value from the first test phase (30 minutes before lunch) was used as the global baseline for rCBFi calculation.

Acknowledgements:
This work is supported by the Engineering and Physical Science Research Council (Grant No. EP/T00097X/1): the Quantum Technology Hub in Quantum Imaging (QuantiC) and the University of Strathclyde. We thank Professor Robert Henderson, University of Edinburgh, for supporting us with the SPAD sensor – ATLAS was designed in a project funded by Reality Labs, Meta Platforms Inc., Menlo Park, CA 94025, USA. We are grateful to STMicroelectronics for CMOS manufacturing of the device within the University of Edinburgh Collaboration Agreement. We also appreciate Dr. Qianqian Fang's support on MC simulations using MCX.

Contact: mingliang.pan@strath.ac.uk; David.Li@strath.ac.uk

P014

Investigating the effects of physiological variables on cerebrovascular reactivity in cerebral small vessel disease

Uffaq Mastoor[1], Michael S. Stringer[1], Keelin Ridge[1], Carmen Arteaga Reyes[1], Oriana Arsenov [1], Una Clancy [1], Maria Valdes Hernandez [1], Dany Jaime Garcia [1], Francesca Chappell [1], Fergus Doubal [1], Michael J. Thrippleton[1], Joanna M. Wardlaw[1], on behalf of the MSS3 study group.

1. Centre for Clinical Brain Sciences, University of Edinburgh, UK

Keywords: cerebrovascular reactivity, cerebral small vessel disease, BOLD MRI

Abstract:

Cerebral small vessel disease (SVD) accounts for approximately 20% of strokes and 45% of dementias, yet its causes remain poorly understood, and there are currently no effective treatments. One promising approach to investigating vascular health in vivo is through magnetic resonance imaging (MRI), including the use of cerebrovascular reactivity (CVR) measurements, which assess the brain's vascular response to a hypercapnic gas challenge. Lower CVR has been linked to more severe SVD and greater disease progression. However, few studies have explored how physiological factors, such as heart and respiration rate, may influence CVR measurements. Addressing this gap is important for improving the reliability of CVR as a clinical tool in SVD research.

Using data from the well-characterized Mild Stroke Study 3 cohort, this study will investigate how cardiac and respiratory variability influence CVR assessment in SVD. We will employ a comprehensive preprocessing pipeline for BOLD MRI data, including slice timing correction, motion correction, and spatial smoothing. Physiological data will be sampled and aligned with the BOLD time series. CVR magnitude will be modelled using the end-tidal CO_2 (ETCO2) trace as the primary regressor, both with and without additional correction for cardiac and respiratory-induced motion. To refine CVR delay estimation, a series of time-shifted ETCO2 regressors will be evaluated, selecting the shift that minimizes residual error. By advancing methods to account for physiological variability in CVR measurement, this work aims to improve the accuracy and interpretability of CVR as a biomarker for SVD. Findings from this study will help inform best practices for neurovascular imaging, with the potential to enhance the clinical utility of CVR in identifying and monitoring individuals at risk of cerebrovascular decline.

All work will be conducted on anonymised data under existing ethical approvals (Southeast Scotland Regional Ethics Committee, reference 18/SS/0044). Findings will be presented at the conference.

Contact: u.mastoor@sms.ed.ac.uk

P015

Incorporating Fluorine Probes in 7T Head Coils for Concurrent Field Monitoring

Eva McEwan[1], Belinda Ding[2], Sydney Williams[3], Shajan Gunamony[1,3]

1. MRCoilTech Limited, Glasgow, UK
2. Siemens Healthcare Limited, UK
3. Imaging Centre of Excellence, University of Glasgow, UK

Keywords: RF coil design, 7T MRI

Abstract:

Following the realisation of a gap in the market for 64-channel receive radiofrequency (RF) coils at 7T MRI as the current industry standard head coil has only 32-receive channels, development began between MRCoilTech, with partners NHS and the University of Glasgow, on an 8Tx64Rx head coil for use in 7T MRI. This coil was successfully delivered, producing higher resolution scans as the increased number of channels produces an improved signal-to-noise ratio (SNR).

However, field fluctuations and system non-linearities at 7T can degrade image quality which must be corrected to fully utilise the improved SNR. As such, MRCoilTech entered a partnership with Skope to incorporate field probes into the coil to create an upgraded coil, the Neurocam 7T™. These fluorine-containing field probes can then be used for dynamic field monitoring and correcting magnetic field perturbations during data acquisition.

This coil followed the design of the current 8 transmit channel and 64 receive channel model, with design updates to allow probe integration. 16-field probes were arranged in a constellation on the surface of the receive helmet such that the probe conditioning is satisfied.

Despite the compact nature of the coil, the fluoride probes and associated electronics were successfully incorporated into the coil. SNR and B_1^+ field measurements were performed in a phantom on a 7T MRI scanner (MAGNETOM Terra, Siemens Healthcare, Germany) before and after integrating the field probes. B_1^+ maps (Fig.1) and SNR maps (Fig.2) demonstrate that the probes have been successfully integrated inside the coil. There is no noticeable interaction between the probes and the RF coil and the coil performance has been retained.

Figures:

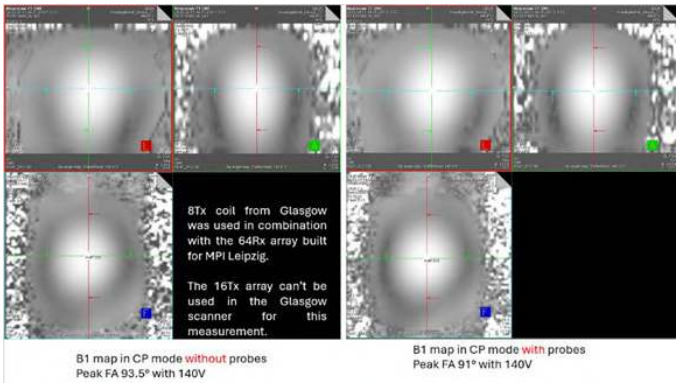

Figure 1: B_1^+ mapping in CP mode of the 8Tx64Rx coil with no probes (left), and with probes incorporated (right)

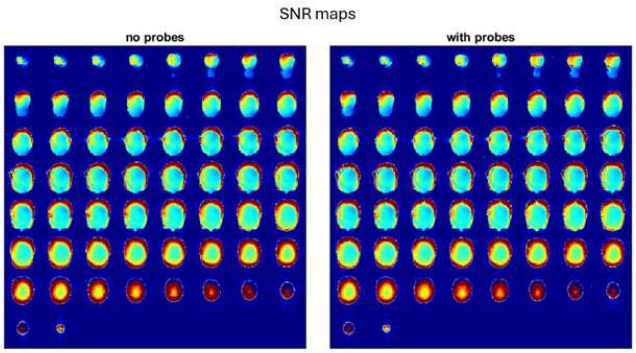

Figure 2: Comparison of the SNR maps of the 8Tx64Rx coil with no probes (left), and with probes incorporated (right)

Contact: eva@mr-coiltech.co.uk / eva.mcewan.2021@uni.strath.ac.uk

P016

T_1 mapping with multi-contrast MP-RAGE at 7T

Janhavi Ghosalkar[1], Graeme A. Keith[1], Belinda Ding[2], Natasha Fullerton[3], Shajan Gunamony[1,4], David Porter[1]

1. Imaging Centre of Excellence, University of Glasgow, Glasgow, Scotland
2. Siemens Healthcare, Camberley, UK
3. NHS Greater Glasgow and Clyde, Glasgow, UK
4. MR CoilTech Limited, Glasgow, UK

Abstract:

Introduction:

This study expands the quantitative capabilities of the MP2RAGE [1] sequence by acquiring additional images at multiple inversion times (TI). Using GRAPPA in two dimensions accelerates data sampling in both phase-encoding directions, reducing overall scan time and sampling time for each image during spin relaxation after the inversion pulse. Unlike previous work [2], with radial readout, this study uses a Cartesian method, a straightforward modification of the standard sequence. The Deichmann-Haase model function [3] used for parameter fitting imperfectly accounts for the incomplete relaxation during the delay time (TD). To address this limitation, an updated model function based on previous work [2] was evaluated in this study.

Methods:

Healthy volunteers were scanned using the sequence on a 7T MAGNETOM Terra MRI scanner (Siemens Healthineers AG, Germany) and a custom-built 8Tx64Rx head coil [4], a 0.86mm^3 isotropic resolution, and TIs ranging from 500ms-3100ms. T_1 fitting was a voxel-wise analysis using the Look-Locker method with Deichmann-Haase correction [3]. Additionally, Monte Carlo simulations were performed in MATLAB to compare the Deichmann-Haase method of T_1 estimation with the updated model function.

Results/Discussion:

Figure 1 shows the different T_1-weighted contrasts from a single acquisition using four TI values. Corresponding T_1 maps are also shown using the three-parameter fitting approach with Deichmann-Haase correction. This model underestimates the mean T_1 value compared to the true 1200ms due to incomplete relaxation of longitudinal magnetization before subsequent inversions, whereas the updated model provides a much closer match. The coefficient of variation is lower with the updated model when a two-parameter fit is performed and greater with a three-parameter fit, which is illustrated in Figure 2. Exploiting this performance of the two-parameter fit by determining the flip angle and inversion efficiency could enhance the accuracy and precision of T_1 estimations in future studies.

References:

[1] Marques JP, Kober T, Krueger G, van der Zwaag W, Van de Moortele PF, Gruetter R. MP2RAGE, a self bias-field corrected sequence for improved segmentation and T₁-mapping at high field. Neuroimage. Jan 2010;49(2):1271-1281. doi:10.1016/j.neuroimage.2009.10.002

[2] Kecskemeti S, Samsonov A, Hurley SA, Dean DC, Field A, Alexander AL. MPnRAGE: A technique to simultaneously acquire hundreds of differently contrasted MPRAGE images with applications to quantitative T₁ mapping. Magnetic Resonance in Medicine. Mar 2016;75(3):1040-1053. doi:10.1002/mrm.25674

[3] Deichmann R, Haase A. QUANTIFICATION OF T1 VALUES BY SNAPSHOT-FLASH NMR IMAGING. Journal of Magnetic Resonance. Feb 1992;96(3):608-612. doi:10.1016/0022-2364(92)90347-a

[4] Williams SN, Allwood-Spiers S, McElhinney P, et al. A Nested Eight-Channel Transmit Array With Open-Face Concept for Human Brain Imaging at 7 Tesla. Frontiers in Physics. Jul 2021;9701330. doi:10.3389/fphy.2021.701330

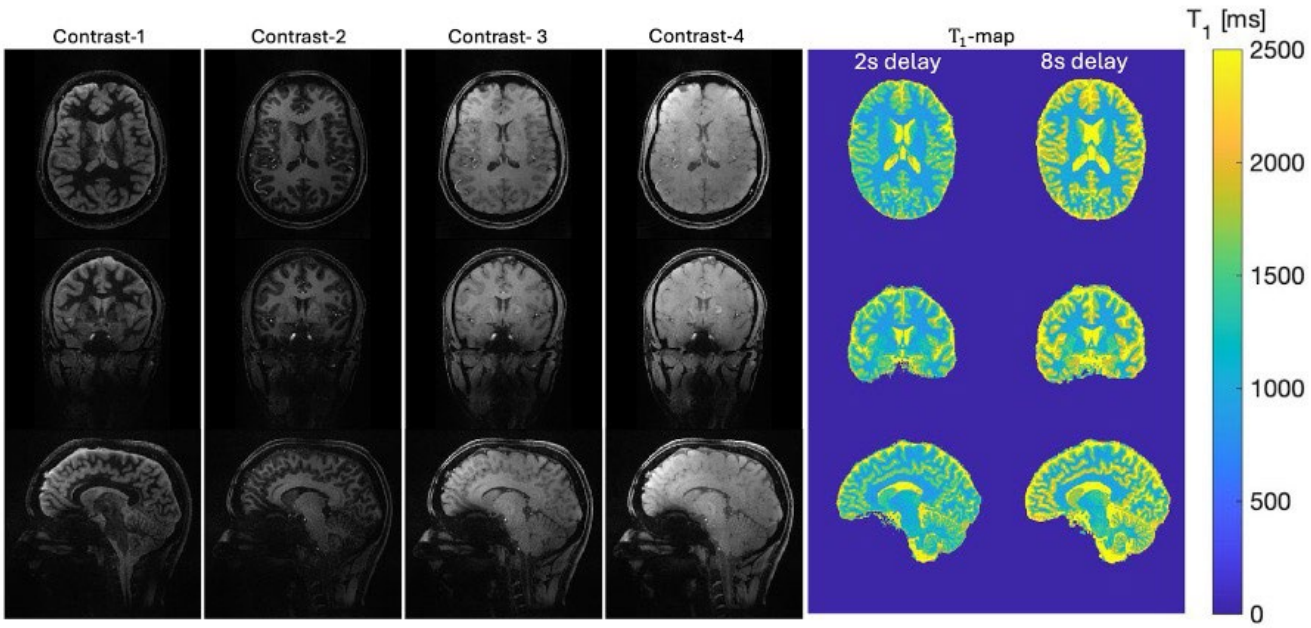

Figure 1: In vivo images showing T_1-w contrasts for four TIs of 506ms, 1343ms, 2180ms, and 3017ms, with a total acquisition time of 7.9 mins, acquired using a GRAPPA factor of 3x2(left). T_1 maps in three planes for two different delay times (TD) with a GRAPPA acceleration factor of 3x2 from the same volunteer(right).

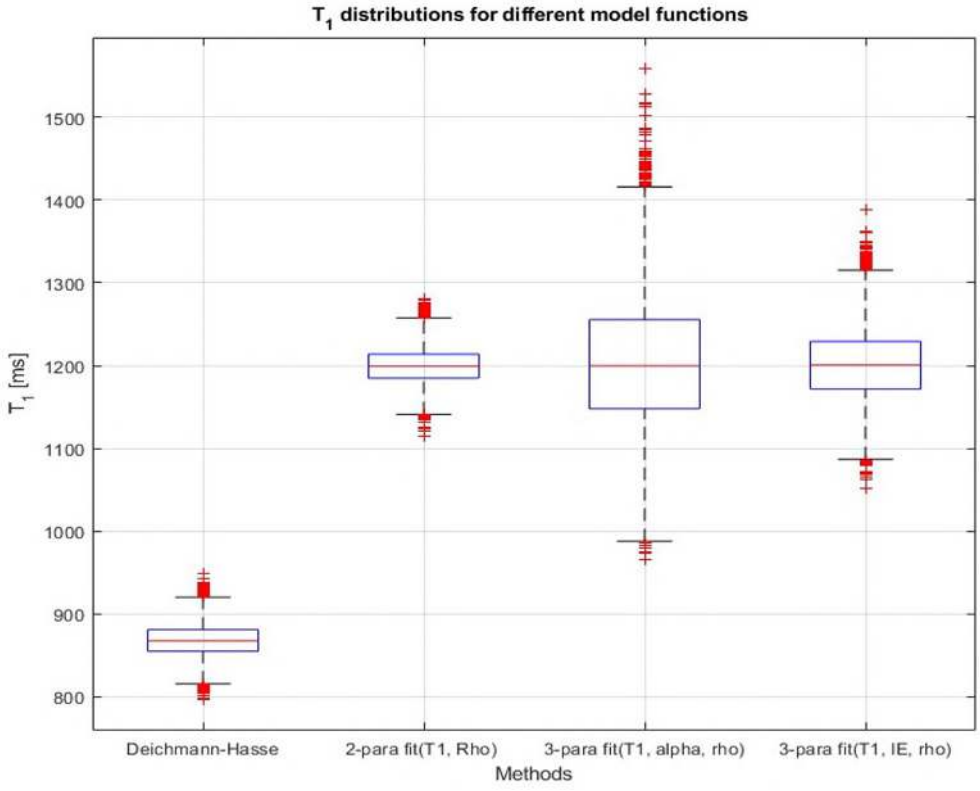

Figure 2: Boxplot(top) showing the results of a 10,000-sample Monte Carlo simulation for two different model functions, with a dotted line at 1200ms showing the value of correct T_1. The two and three-parameter fitting models use the updated model function. The mean and standard deviations of each model are 867.6±19.4ms, 1199.6 ± 21.5ms, 1203.6 ± 81ms, and 1201.7 ± 42.9ms (left to right).

P017

Prospective 8Tx thoracic-lumbar spinal array at 7T MRI

Yiling Hu[1], Divya Baskaran[1], Belinda Ding[2], David A. Porter[1], Natasha Fullerton[3], Shajan Gunamony[1,4]

1. Imaging Centre of Excellence, University of Glasgow, Glasgow, UK
2. Queen Elizabeth Hospital, University Hospitals Birmingham NHS Foundation Trust, UK
3. Queen Elizabeth University Hospital, NHS Greater Glasgow and Clyde, UK
4. MR CoilTech Limited, Glasgow, UK

Keywords: transmit coil design, spinal imaging, ultra-high-field MRI

Abstract:

7T MRI offers superior resolution but has increased radiofrequency (RF) field inhomogeneity and tissue heating [1]. Parallel transmission (pTx) addresses this by splitting the transmit coil into multiple independently-controlled channels [2]. This abstract presents preliminary simulation results from a new pTx spinal array design with eight transmit elements for thoracic-lumbar spinal imaging, and compares it with an existing design modelled after Kraff et al. [3].

Finite-difference time-domain (FDTD) EM simulations of an eight-channel transmit array were performed in CST 2022. The array is composed of copper wire loops arranged in a dual-column configuration, with nearest-neighbor overlap-decoupling and next-nearest-neighbor inductively decoupling. Loops have fixed capacitors of 6.8 pF to 7.5 pF and ports for matching, tuning, and decoupling. Scanner conditions were recreated using a copper EM shield, copper bore, and coil housing. The array's right column is 180° phase shifted from the left column. B_1^+ and SAR simulations were performed on a muscle phantom and a Duke digital voxel model, respectively. This non-offset array was compared to an offset design similar to Kraff's. The offset array used overlap-decoupling with all elements placed in the same plane using jumper cables.

Overlap dimensions for the non-offset array were optimized as 30mm between left and right columns, 14-18mm between vertically adjacent elements. Both reflection and coupling coefficients were tuned and matched to below -20dB and -15dB, respectively. The non-offset coil has a more uniform B_1^+ excitation field, higher B_1^+ average (1.50µT), and more uniformly distributed SAR compared to the offset coil (B_1^+ average of 1.09µT).

FDTD EM simulations of a prospective dual-column 8Tx array for thoracic-lumbar spinal imaging yield improved B_1^+ field distribution compared to an existing design. Developing a 4Tx cervical-thoracic spine coil to the 8Tx array using channel splitters would provide a better picture of whole-spine imaging.

References: [1] Williams et al. (2023). Physics in Medicine and Biology, 68(2). [2] Padormo et al. (2016). NMR in Biomedicine, 29(9), 1145–1161. [3] Kraff et al. (2009). Invest. Radiol, 44(11), 734-740.

Contact: y.hu.5@research.gla.ac.uk

Figures

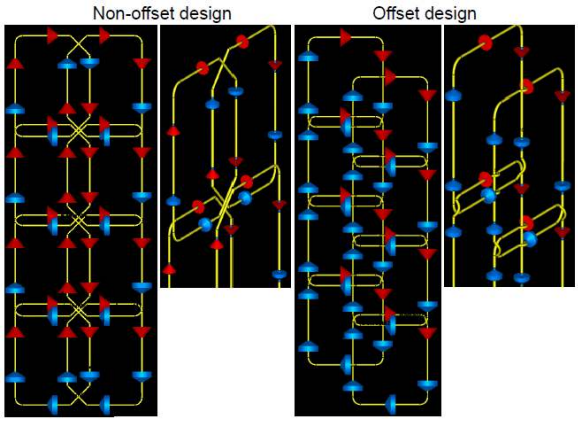

Figure. 1. Non-offset (left) and offset (right) coil layouts.

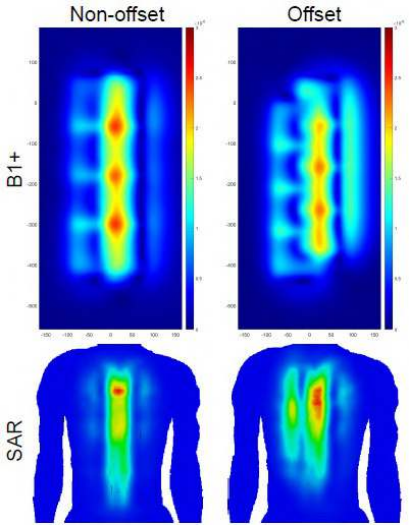

Figure. 2. B1+ (top) and SAR (bottom) maps of non-offset (left) and offset (right) arrays. B1+ maps are scaled to a maximum of 3μT.

P018

Hypoxia and Vascular Phenotypes in TNBC Xenografts: A Platform for Imaging-Based Evaluation Using Size-Fractionated Microbubbles

Anggraeni Ayu Rengganis[1,2*], Kirsteen Campbell[1,2], Karen Blyth[1,2], Emma Brown[1,2], Algernon Bloom[1,2], Colin Nixon[2], Barbara Cadden[2], Helen Mulvana[3], David Y. Lewis [1,2]

1. College of Medical, Veterinary, and Life Science, University of Glasgow, UK
2. Cancer Research UK – Scotland Institute, Glasgow, UK
3. James Watt School of Engineering, University of Glasgow, Glasgow, UK

Keywords: vascular phenotype, hypoxia, microbubbles, contrast enhanced ultrasound imaging (CEUS), TNBC (Triple-negative Breast Cancer)

Abstract:

Triple-negative breast cancer (TNBC) is a heterogeneous and aggressive disease with limited targeted therapy options. Differences in vascular phenotype and hypoxia among TNBC subtypes may offer valuable insights for imaging-based monitoring. While markers such as CD31, α-SMA, and CAIX assess - vascular pathology, their *in vivo* imaging correlates remain poorly understood. Ultrasound contrast agents (UCAs), particularly microbubbles, offer a promising non-invasive method to probe tumour vasculature. We are therefore investigating the impact of microbubble size distribution on acoustic imaging efficacy validated to underlying vascular pathology.

We established xenograft tumours using MDA-MB-231 (highly invasive) and MDA-MB-468 (less invasive) TNBC cell lines in female mice (n = 4 per group). Tumours were analysed histologically using H&E and immunohistochemistry for CD31, α-SMA, and CAIX. Vessel characteristics and hypoxia were quantified using HALO v3.6 image analysis software. Statistical comparisons were performed using unpaired t-tests. In parallel, we studied on microbubble size fractionation using low g-force centrifugation to optimize size-specific vascular imaging for future in vivo applications.

Vessel density did not differ significantly between the two tumour types. However, MDA-MB-468 tumours exhibited smaller vessel diameters (mean 27.21 µm vs. 34.32 µm, $p < 0.05$), lower α-SMA positivity, (15.20% vs. 19.59%, $p < 0.05$), and higher hypoxia (CAIX positivity: 44.40% vs. 28.04%, p 0.10), indicating vessel immaturity and reduced perfusion in the less invasive tumour. Preliminary results from size-fractionation of SonoVue (Bracco S.A.) microbubble suspensions showed that two populations: a near-homogeneous population of smaller microbubbles (<1.5 µm) and larger bubbles (>2 µm).

This study highlights key vascular and hypoxic differences between TNBC tumour models and establishes a biological foundation for future contrast-enhanced ultrasound imaging. We will determine the acoustic behaviour for each microbubble size fraction and establish the acoustic imaging phenotypes in orthotopic breast cancer models with differing aggressivity to determine the imaging sensitivity to vascular dysfunction.

Acknowledgements:
This work is supported by Indonesia Endowment Fund for Education (LPDP), Ministry of Finance, Republic of Indonesia and funding from Cancer Research UK for core funding to the CRUK Scotland Institute (A13827) and to David Lewis' laboratory (A25006).

Contact: a.rengganis.1@research.gla.ac.uk

P019

Deep Learning for Cardiac MRI: Current Evidence on Clinical Integration for Segmentation, Prediction, and Diagnosis.

Systematic Review and Meta Analysis.

Fatemah Aladwani*[1], Alessandro Perelli[2], Ify Mordi[1], Faisel Khan[1]

1. Department of Cardiovascular Research, School of Medicine, University of Dundee, UK
2. Division of Biomedical Engineering, School of Science and Engineering, University of Dundee, UK

Keywords: Deep Learning, Cardiac MRI, Segmentation, Diagnosis, Prediction

Abstract:

Cardiac magnetic resonance imaging (CMR) is the gold standard for evaluating cardiovascular disease (CVD), offering unmatched precision in functional and structural cardiac assessment. While deep learning (DL) techniques have shown promise in automating aspects of CMR image analysis, their real-world clinical translation remains under investigation. This systematic review and meta-analysis critically assess the current literature on DL applications in CMR, specifically in segmentation, diagnosis, and prediction.

A comprehensive literature search was performed across Medline, Web of Science, Embase, and Scopus for studies published between 2020 and August 1, 2023. Eligible studies employed DL techniques for CMR-based segmentation, diagnosis, or outcome prediction. Meta-analysis was conducted using MetaDisc version 1.4. Statistical significance was defined as $p < 0.05$, with an $I^2 \geq 75\%$ indicating substantial heterogeneity.

Out of 872 identified articles, 45 met the inclusion criteria: 38 focused on segmentation, 5 on diagnosis, and 2 on prediction. Supervised learning dominated the field (93.6%), with U-Net being the most frequently used architecture (63.8%). The mean Dice Similarity Coefficient (DSC) reported across 11 studies was 0.91 ± 0.03. Hausdorff distance (HD), reported in 5 studies, averaged 9.89 ± 6.45. Pooled diagnostic metrics showed high performance with a sensitivity of 95% (95% CI: 91–97%) and specificity of 90% (95% CI: 88–93%). Segmentation tasks demonstrated even higher accuracy, with pooled sensitivity and specificity reaching 100% (95% CI: 99–100%) and 98% (95% CI: 98–99%), respectively. The average CLAIM (Checklist for Artificial Intelligence in Medical Imaging) score across studies was 86.3%, reflecting strong methodological quality.

DL-based approaches show robust performance in CMR segmentation and diagnostic tasks, often matching or surpassing manual analysis. These findings highlight DL's potential to enhance clinical decision-making, although further validation is needed for broader clinical adoption.

Contact: Fatemah Aladwani: 2429072@dundee.ac.uk

P020

Facilitating Early Diagnosis of Neurodegenerative Diseases through Normative Modelling of Healthy Brain States

Mihaela Lyutskanova[1], Christian Keitel[1], Tom Gilbertson[2], Douglas Steele[2], Christopher Benwell[1]

1. Division of Psychology, School of Humanities, Social Sciences and Law, University of Dundee, Dundee, UK
2. Imaging Science and Technology, School of Medicine, University of Dundee, Ninewells Hospital, Dundee, UK

Relevant Keywords: Parkinson's Disease, EEG, Apathy, Decision-making, Normative modelling

Abstract:

Parkinson's Disease (PD) affects 10 million people worldwide. It is the fastest growing neurodegenerative disease (Feigin et al., 2019) and diagnosis is often delayed. Apathy, a non-motor symptom of PD, is characterized by reduction of voluntary goal-directed behaviour (Levy & Dubois, 2006). It predicts early cognitive decline (Martin et al., 2019) and is associated with an almost 3-fold increased risk of mortality (Le Heron et al., 2024).

This research project aims to improve early PD diagnosis by testing brainwave-based biomarkers detectable before visible symptoms. Crucially, early diagnosis will improve patients' quality of life by allowing for early interventions, life adjustments, and a more favourable disease progression. This study will also extend understanding of cortical regions and mechanisms underpinning apathy through a decision-making paradigm.

Recent studies suggest that electroencephalography (EEG) is a promising tool in detecting PD biomarkers, even in early stages of the disease (Gimenez-Aparisi et al., 2023). Our project builds upon recent methodological and theoretical advances to improve early detection of PD-related neuropathology through EEG-recorded brainwaves.

Using existing datasets from >1000 healthy controls, we aim to develop normative models of EEG measures as a function of age, sex, and cognitive abilities. These models will be tested with data from 60 PD patients with minimal motor symptoms to assess how well they are differentiated from healthy controls. The richer information from EEG-based normative models will enhance diagnostic sensitivity and specificity compared to classic case-control studies.
Moreover, 60 PD patients are taking part in an EEG experiment to test their decision-making skills. PD-related deficits in decision-making have been shown to predict the symptom burden of apathy (Gilmour et. al., 2023). We will test whether changes in decision-related EEG signatures may represent novel PD biomarkers that track symptom severity.

We are currently collecting data and preliminary results will be available soon.

Acknowledgements:
This work is supported by TENOVUS Scotland and the Scottish Neurological Research Fund.

Contact: 180006960@dundee.ac.uk

P021

Relationships between brain structure and autistic characteristics across restoration of weight from anorexia nervosa: a longitudinal neuroimaging study

Michelle Sader[1,2], Daniel Halls[3], Jess Kerr-Gaffney[2,4], Gordon D. Waiter[1,2], Karri Gillespie-Smith[2,5], Fiona Duffy[2,5,6], Kate Tchanturia[2,4,7]

1. School of Medicine, Medical Sciences and Nutrition, University of Aberdeen, Scotland, UK
2. Eating Disorders and Autism Collaborative (EDAC), University of Edinburgh, Scotland, UK
3. Computational Neuroimaging Laboratory, University of Nottingham, UK
4. Department of Psychological Medicine, King's College London, UK
5. School of Health in Social Science, University of Edinburgh, Scotland, UK
6. NHS Lothian Child and Adolescent Mental Health Services, Royal Edinburgh Hospital, Scotland, UK
7. Illia State University, Department of Psychology, Tbilisi, Georgia

Keywords
Anorexia nervosa, autism, body mass index, weight restoration, magnetic resonance imaging

Abstract

Background:

Common neuroanatomical regions are associated with both states of anorexia nervosa (AN) and autistic characteristics, but recent research suggests that autistic characteristics and regions of the brain associated with these characteristics in acute AN (ac-AN) are unrelated to BMI. This study aims to examine neural correlates associated with longitudinal relapse and weight restoration from ac-AN.

Methods:

In total, 79 individuals (Healthy Controls [HC]=23; nRelapsed=21; nWeight Restored [WR]=35) from the Brain imaging of Emotion And Cognition of adolescents with Anorexia Nervosa (BEACON) study were included, with T1-weighted brain scans obtained across a three-year time period. Mean change (Δ) in sociodemographic characteristics and structural parameters were compared between groups. To further examine the relationship between autistic characteristics, brain structure and BMI, linear associations between Δ brain morphology and autistic characteristics were compared between HCs, those WR and those who relapsed.

Results:

In those who relapsed, Δ volume of the MFG significantly differed between HC individuals (*t=-2.814; p=0.00554*), but not WR individuals. Relationships between Δ brain morphology and presentation of autistic characteristics significantly differed between HCs and WR individuals in the anterior cingulate cortex (ACC) (*β=1.81; p=0.0237*), and between WR individuals and those who experienced AN relapse in the white matter of the CB (*β=-1.80; p=0.035*).

Conclusion:

Findings suggest that the relapsed and WR brain demonstrate differential growth and structural relationships with autistic characteristics relative to brains of individuals with no history of an AN.

Images/Figures

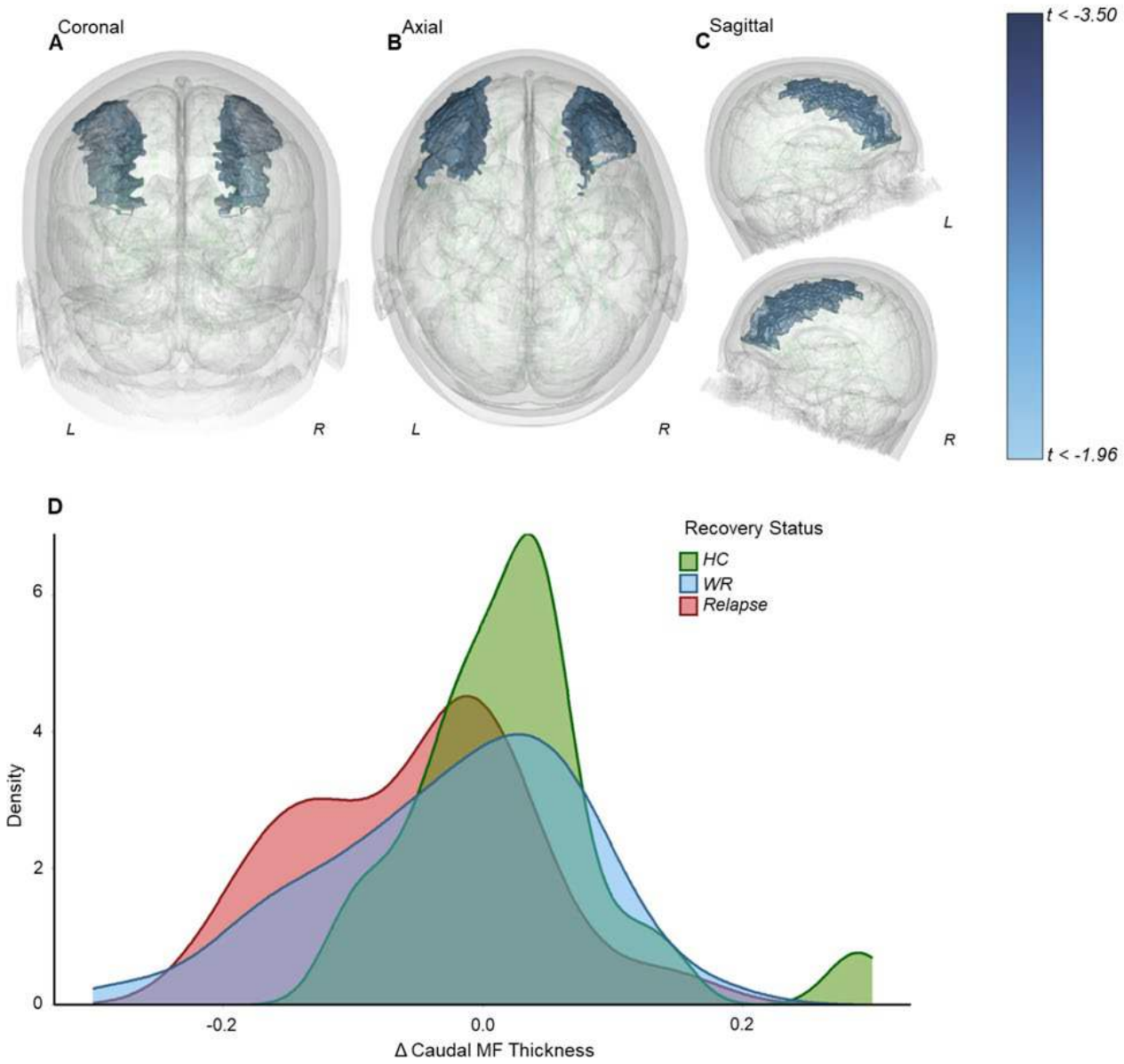

Figure 1. A-priori differences in Δ MFG cortical thickness between those who experienced AN relapse (n=21) and HCs (n=23) in coronal (A), axial (B) and sagittal (C) orientations. A density plot (D) compares the distribution of Δ MFG thickness between groups, with Δ thickness in HC, WR and individuals experiencing relapse in green, blue and red respectively.

[Abbreviations: HC – Healthy Controls; L – Left; MF – Middle Frontal; R – Right; WR – Weight Restored]

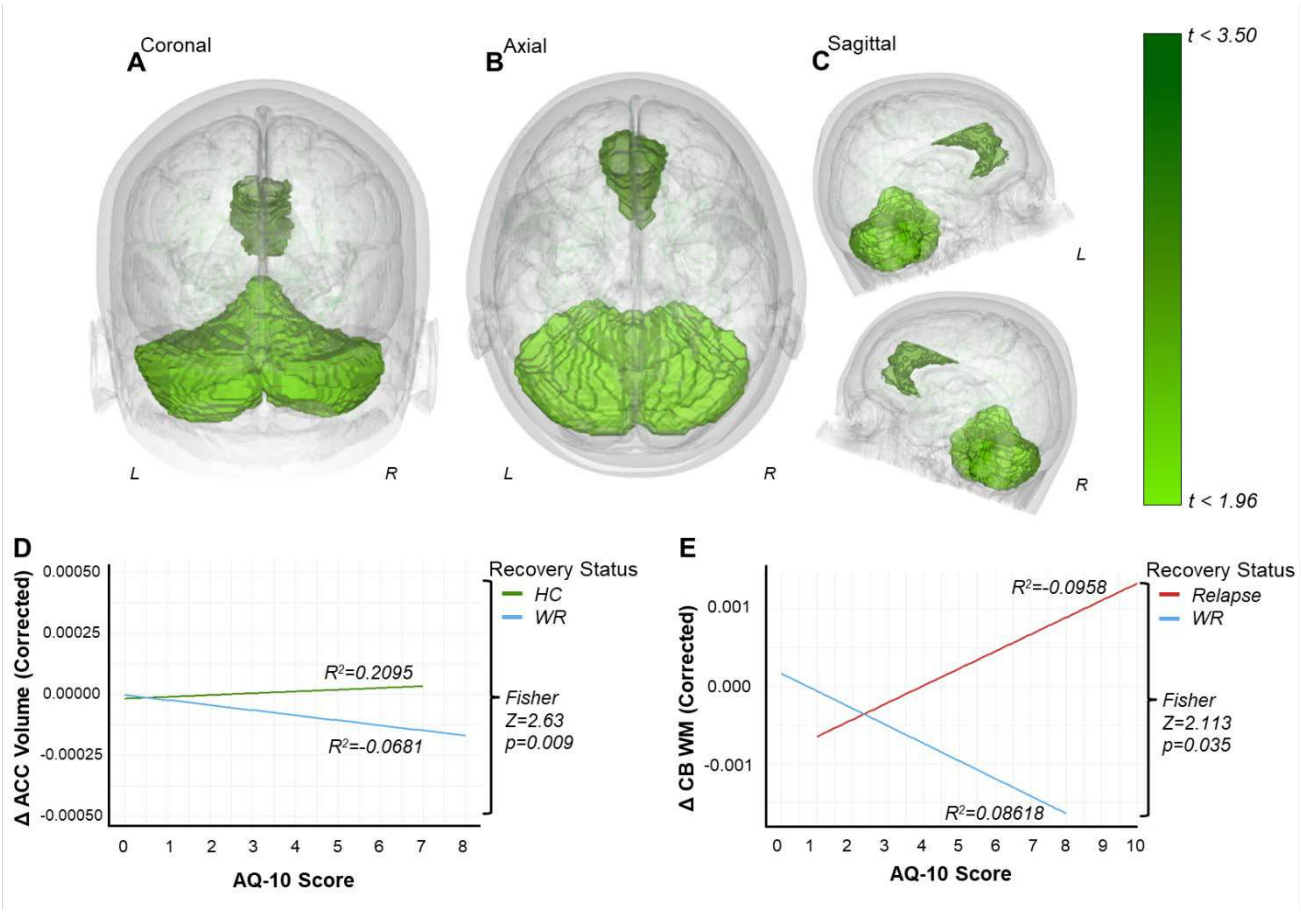

Figure 2. A-priori regions displaying a significant difference in slope when visualising relationships between Δ structure and AQ-10 scores between HCs (n=21), WR individuals (n=35) and those experiencing AN relapse (n=21). Images are displayed in coronal (A), axial (B) and sagittal (C) orientations. Linear models display a significant difference in slope between Δ ACC volume and AQ-10 scores (D) and Δ CB WM and AQ-10 scores (E). Relationships between Δ ACC volume and AQ-10 scores significantly differed between HCs and WR individuals, while relationships between Δ CB WM And AQ-10 scores differed between WR individuals and those who relapsed.

[Abbreviations: HC – Healthy Controls; L – Left; MF – Middle Frontal; R – Right; WR – Weight Restored]

Acknowledgements

This work was made possible by funding for the BEACON study, provided by the MRC-MRF Fund (MR/S020381/1; BiomaRkers for Anorexia Nervosa and autism spectrum Disorders – longitudinal study and MR/R004595/1; The Triple A study [Adolescents with Anorexia and Autism]: A search for biomarkers). Additionally, M.S., J.K.G, G.W., K.T., K.G.S. and F.D. are supported by UK Research and Innovation (MRC, ESRC, AHRC), the National Institute for Health and Care Research and the Medical Research Foundation as part of the Eating Disorders and Autism Collaborative (EDAC) network (grant number: MR/X03058X/1). For the purpose of open access, the authors have applied a Creative Commons Attribution (CC BY) licence to any Author Accepted Manuscript version arising from this submission. K.T. would like to acknowledge the National Institute for Health and Care Research (NIHR) Maudsley Biomedical Research Centre (BRC). The views expressed are those of the author(s) and not necessarily those of the NHS, the NIHR or the Department of Health and Social Care.

Contact: michelle.sader3@abdn.ac.uk

P022

Challenges in Segmenting Lesions in Breast Ultrasound Images

Aamal Alghamdi[1*], Mohamed Elawady[1], Andrew Abel [1]

1. Department of Computer and Information Sciences, University of Strathclyde, Glasgow, UK

Keywords: image segmentation, breast ultrasound, pattern recognition, medical imaging, deep learning.

Abstract:

Breast ultrasound imaging is broadly applied for the early detection and diagnosis of breast lesions. Ultrasound imaging is a non-invasive tool and is suitable for dense breast tissues. It has a relatively low cost and provides real-time visualization. Despite these advantages, ultrasound imaging also presents certain limitations. These limitations include low signal-to-noise ratio, speckle noise, low contrast, blurred edges, and the heterogeneous appearance of lesions. They are compounded by varying image acquisition conditions and subjective interpretations, making accurate lesion segmentation significantly challenging. In this work, we evaluate the model performance of four widely used deep-learning segmentation models (Unet, Unet++, FPN, Deeplabv3+) on two public breast ultrasound datasets (UDAIT and BUSIS). These datasets largely consist of images without embedded biomarkers, textual overlays, or visual artifacts. We present both quantitative results—using metrics such as the Dice coefficient, Jaccard index, Recall, Specificity, and Precision—and qualitative comparisons through visual inspection of segmentation maps. This study provides valuable baseline comparisons and highlights key limitations in current approaches.

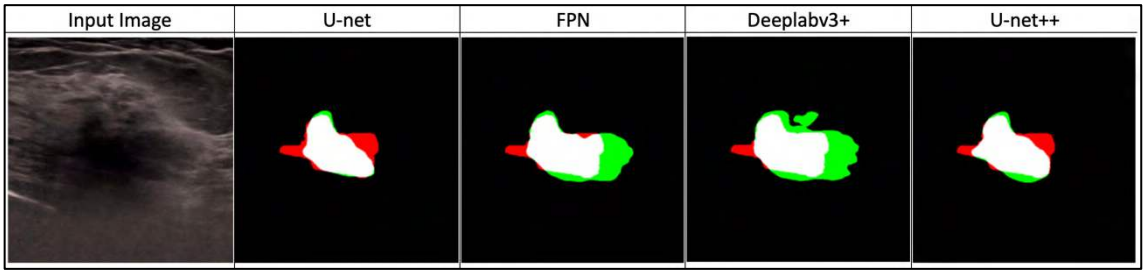

Figure 1: Comparison of breast lesion segmentation results from a sample of the BUSIS dataset. The green color represents the false positive, while the red represents the false negative.

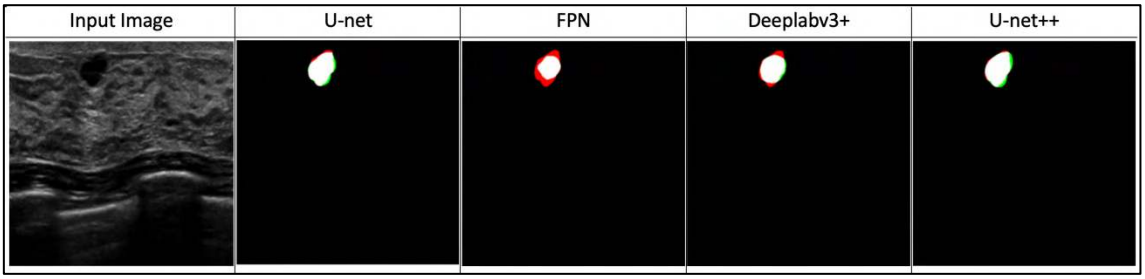

Figure 2: Comparison of breast lesion segmentation results from a sample of the UDIAT dataset. The green color represents the false positive, while the red represents the false negative.

Contact: aamal.alghamdi@strath.ac.uk

P023

Prospective Assessment of Survival Outcomes in Men Over 80 Undergoing Transrectal Ultrasound-Guided Prostate Biopsy

Dareen Alghamadi [1]

1. University Of Dundee

Abstract:

Introduction:

Prostate cancer is the second most common malignancy among elderly men in Western countries. Transrectal ultrasound (TRUS)-guided biopsy remains a key diagnostic tool; however, it carries significant risks, especially in older patients. These risks include complications such as sepsis, acute urinary retention, and rectal bleeding, which can contribute to increased morbidity and mortality. This study aimed to assess cancer-specific survival in men over 80 years old and determine whether undergoing TRUS biopsy provides any survival benefit.

Methods:

From January 2005 to December 2015, we analyzed outcomes in 200 patients (median age: 82 years) who underwent TRUS biopsy due to elevated prostate-specific antigen (PSA) levels (>4.0 ng/mL) and/or abnormal digital rectal examination (DRE). Patients were tracked until death using an electronic database and a unique identifier within a defined geographical region. Cancer-specific and overall survival were analyzed using SPSS, while R Project was utilized to develop and assess two nomograms for predicting survival duration and post-biopsy mortality risk. Statistical significance was set at $p < 0.05$.

Results:

At the end of follow-up, only 24 patients remained alive (median age: 91 years). PSA levels ranged from 4.88 to 102.7 ng/mL. Log-rank and Breslow tests demonstrated that elevated PSA, metastases, and ISUP grade 8–10 were linked to shorter survival. Age, comorbidities, and tumor type were included in the nomogram due to their clinical relevance. Patients younger than 81 years had lower mortality risk, whereas those older than 88 faced higher risks. Biopsy-related complications increased mortality in both malignant and benign cases, and metastasis significantly worsened survival. However, comorbidities did not impact survival probability.

Conclusions:

Our findings highlight that advanced age (≥80 years), high Gleason score, metastases, and elevated PSA predict worse survival outcomes following TRUS biopsy in elderly men.

P024

Ultrasound Technology for Wearable Imaging: Rigid vs Flexible Arrays

Xanthe Miller[1], Hilde Metzger[1], Emma Harris[2] and Sandy Cochran[1]

1. Centre for Medical and Industrial Ultrasonics, James Watt School of Engineering, University of Glasgow, UK
2. Institute for Cancer Research, Centre for Cancer Imaging, Sutton, UK

Keywords: wearable ultrasound, flexible ultrasound, imaging

Abstract:

Wearable ultrasound imaging is an emerging and increasingly relevant technology for biomedical imaging. There are various approaches to developing high quality wearable ultrasound imaging devices, which can be broadly divided into those based on traditional, rigid ultrasound arrays and those using emerging flexible ultrasound arrays. Both are subject to advantages and disadvantages. The more traditional rigid devices benefiting from extensive existing knowledge, sophisticated technologies and advanced imaging techniques but are limited by their inability to conform to the contours of human anatomy. Flexible arrays gain in conformability but face challenges in image reconstruction and image quality.

Two high frequency ultrasound linear arrays are compared in this study. The first is a lead-free flexible array (Novosound, Newhouse, UK), Fig (a). This is a 32-element array comprising a metal substrate with proprietary thin-film piezoelectric deposition as the active material. The array has a centre frequency of 25 MHz, and the element pitch is 0.3 mm. The second array is a rigid 128-element array (Vermon, Tours, Francs) using a proprietary single-crystal piezocomposite technology with a centre frequency of 28 MHz and a pitch of 0.07 mm, pictured in Fig (b).

The arrays are controlled using a Verasonics Vantage 128 and are connected via flexible PCBs with custom interposers to enable implementation of standard ultrasound array characterisation techniques. Impedance plots for the flexible array and the rigid array are shown in Figs (c) and Fig (d) respectively. Fig (d) shows a more defined prominence compared to Fig (c), suggesting the possibility of poorer transmission from the flexible array, albeit with a wider bandwidth. This is corroborated by measurements made in phantoms and *ex vivo* tissue.

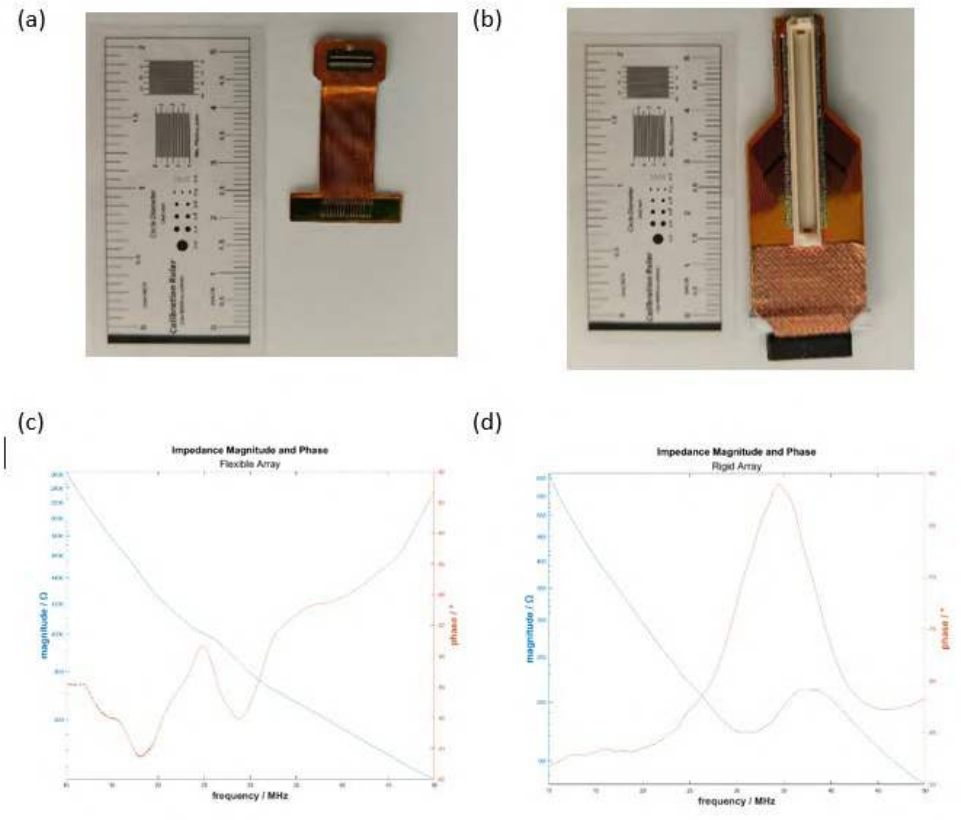

Contact: x.miller.1@research.gla.ac.uk

P025

Compact cerebral blood flow sensing with real-time analysis

Quan Wang,[1]Chenxu Li,[1] **Mingliang Pan,[1]** Ahmet T. Erdogan,[2] Yuanyuan Hua,[2] Neil Finlayson,[3] Robert K. Henderson,[2]and David Day-Uei Li[1]

1. University of Strathclyde, Department of Biomedical Engineering, Glasgow, UK
2. University of Edinburgh, School of Engineering, Integrated Nano and Micro Systems (IMNS), Edinburgh, UK
3. Singular Photonics Ltd., Edinburgh, UK

Keywords: cerebral blood flow, diffuse correlation spectroscopy, single-photon avalanche diodes

Abstract:

Cerebral blood flow (CBF) is a vital biomarker of brain health, intimately linked to neuronal metabolism and neurovascular coupling. Real-time, non-invasive monitoring of CBF is essential for the diagnosis and management of neurological conditions including stroke, traumatic brain injury, and neurodegenerative disorders. Diffuse correlation spectroscopy (DCS) offers a non-invasive approach to probe microvascular dynamics deep within tissue. However, conventional DCS systems remain constrained by hardware bottlenecks—particularly bulky correlator boards and software-based autocorrelation—which limit their speed, sensitivity, and suitability for bedside or ambulatory use.

Innovation:

We present a portable DCS platform powered by **a 512 × 512 SPAD (single-photon avalanche diode) array, ATLAS,** with integrated on-chip autocorrelators. This fully parallelised, compact design enables unprecedented speed and depth sensitivity for real-time CBF monitoring, overcoming the limitations of traditional avalanche photodiode (APD)-based systems.

Methods:

We evaluated SPAD-DCS through phantom testing, vascular occlusion studies, and in vivo cerebral measurements (on human volunteers) against a commercial DCS system. CBF dynamics were measured during baseline and cognitively active conditions (video gaming) to assess functional sensitivity and temporal resolution.

Results:

The prototype achieved robust CBF monitoring at source-detector separations $\boldsymbol{\rho \sim 50}$ **mm**, with a high temporal sampling rate of **56.3 Hz**. In vivo measurements captured **pulsatile flow signals** and **task-evoked CBF changes** in the prefrontal cortex, highlighting its potential for functional neuroimaging. Compared to traditional APD-DCS systems, SPAD-DCS demonstrated a **> 571× improvement in signal-to-noise ratio (SNR)** at ρ = 20 mm in phantom studies.

Impact:

Our DCS system's high sensitivity, extended depth range, and compact form factor make it ideal for clinical neuromonitoring, brain-computer interfaces, and neuroscience research.

We will demonstrate our working CBF prototype live at the conference and invite interest from clinicians, neuroscientists, and potential investors. We aim to accelerate the translation of this breakthrough technology toward bedside, wearable, and brain-machine interface applications.

Acknowledgements:
This work has been funded by the Engineering and Physical Science Research Council (EP/T00097X/1 and EP/T020997/1): the Quantum Technology Hub in Quantum Imaging (QuantiC), the InlightenUs project, the University of Strathclyde, and China Scholarship Council. ATLAS was designed in a project funded by Reality Labs, Meta Platforms Inc., Menlo Park, CA 94025, USA. We are grateful to STMicroelectronics for CMOS manufacturing of the device within the University of Edinburgh Collaboration Agreement.

Contact: David.Li@strath.ac.uk